Extracellular ISG15 triggers ISGylation via a type-I interferon independent mechanism to regulate host response during virus infection

Lindsay Grace Miller[1&], Kim Chiok[1&], Charles Mariasoosai[5], Indira Mohanty[1], Sudiksha Pandit[1], Liyon Mehari[1], Arthur L. Haas[2], Senthil Natesan[5*], Tanya A. Miura[3,4*] Santanu Bose[1*#]

[1]Department of Veterinary Microbiology and Pathology, College of Veterinary Medicine, Washington State University, Pullman, WA 99164, USA

[2] Department of Biochemistry and Molecular Biology, Louisiana State University School of Medicine, New Orleans, LA70313, USA

[3]Department of Biological Sciences, University of Idaho, Moscow, ID 83844, USA

[4]Institute for Modeling Collaboration and Innovation, University of Idaho, Moscow, ID 83844, USA

[5]Department of Pharmaceutical Sciences, College of Pharmacy and Pharmaceutical Sciences, Washington State University, Spokane, WA, 992020, USA

[#]corresponding author: santanu.bose@wsu.edu

[*]senior authors

[&]Equal first authors

Abstract

Type-I interferons (IFN) are key antiviral factors that induce several cellular proteins with antiviral activity. One such protein is Interferon Stimulated Gene 15 (ISG15). ISG15 is conjugated to proteins during ISGylation to confer antiviral activity. Apart from ISGylation, unconjugated ISG15 is also released from cells during immuno-stimulation and virus infection. The role of extracellular ISG15 during virus infection was unknown. We now show that extracellular ISG15 acts as a soluble antiviral factor to restrict virus infection in human epithelial cells via an IFN-independent mechanism. Additionally, we demonstrated that extracellular ISG15 induces expression of intracellular ISG15 and ISGylation in the absence of IFN. Mechanistic studies revealed that extracellular ISG15 interacts with cell surface integrin ($\alpha5\beta1$ integrins) molecules via its RGD-like motif to activate the integrin-FAK (Focal Adhesion Kinase) pathway resulting in IFN-independent ISGylation. Thus, our studies have identified ISG15 protein as a new soluble factor that confers IFN-independent antiviral activity by inducing ISGylation. Additionally, we have unfolded an IFN-independent non-canonical ISGylation by extracellular ISG15 that operates via the integrin-FAK pathway.

Introduction

Type-I Interferons (IFN) mediate antiviral responses via induction of effectors known as Interferon-Stimulated Genes (ISGs)[1]. Interferon Stimulated Gene 15 (ISG15) is an ISG involved in antiviral response and immunomodulatory activity[2]. ISG15 is post-translationally conjugated to host and viral proteins by three ubiquitin-like conjugating enzymes (UBE1L, UBCH8 and HERC5) in a process known as ISGylation[3–5]. Although ISGylation occurs in the cytoplasm, several studies have observed the release of unconjugated monomeric ISG15 protein into the extracellular milieu[6,7,8]. Soluble, extracellular ISG15 promotes proliferation of and exerts cytokine-like activity in immune cells (natural killer cells, PBMCs, T cells) that culminates in IFN-γ production[6,8].

Although viral (influenza A virus[11], SARS-CoV-2[10,11] and rhinovirus[12]) infection triggers extracellular release of ISG15 from infected cells, the role of extracellular ISG15 during virus infection is not well understood. Furthermore, the virus-associated mechanisms by which infection triggers the release of ISG15 and whether extracellular ISG15 has direct antiviral activity during virus infection remain unknown. Although ISG15 is an IFN-stimulated gene, our current study surprisingly revealed that extracellular ISG15 induces an increase in intracellular ISG15 and subsequent ISGylation via an IFN-independent mechanism. Intriguingly, by using two clinically relevant respiratory RNA viruses, Respiratory Syncytial Virus (RSV) and SARS-CoV-2, we show that extracellular ISG15 possesses antiviral activity and can restrict virus infection independent of IFN. Mechanistically, extracellular ISG15 interacted with the cell surface α5β1 integrin to induce intracellular ISG15 protein and ISGylation in target cells via an integrin- Focal Adhesion kinase (FAK) pathway. We also identified the S protein of SARS-CoV-2 as a key viral factor involved in stimulating ISGylation and ISG15 release. Thus, we have identified extracellular ISG15 as a new soluble antiviral factor and further mechanistic studies unfolded a novel IFN-independent antiviral response by extracellular ISG15, which is mediated by integrin-FAK signaling.

Results

SARS-CoV-2 S protein induces intracellular ISG15, ISGylation, and extracellular release of ISG15 in epithelial cells

SARS-CoV-2 inhibits ISGylation response in infected myeloid immune cells (macrophages) due to the activity of the virally encoded ISGylation antagonist, PLpro. The PLpro removes conjugated ISG15 from its cellular target[10,13]. In infected macrophages, the PLpro de-ISGylase activity leads to loss of ISGylation and release of ISG15 into the extracellular milieu[11]. However, whether non-myeloid epithelial cells infected with SARS-CoV-2 undergo ISGylation and release of ISG15 is unknown. This is an important question since, unlike epithelial cells, macrophages do not support productive SARS-CoV-2 infection[14]. Therefore, we aimed to determine whether infection with SARS-CoV-2 resulted in ISGylation and extracellular release of ISG15 from epithelial cells. We infected human lung epithelial Calu-3 cells with SARS-CoV-2 and examined ISGylation-ISG15 dynamics by immunoblotting with anti-ISG15 antibodies (Fig. 1A). As expected, ISGylation was not evident at 48hpi. Remarkably, ISGylation was readily detected in SARS-CoV-2 infected cells at 120hpi (Fig. 1A). ISGylation status in infected cells co-related with PLpro expression, since in contrast to 48hpi, PLpro was undetectable at 120hpi (Fig. 1A). Immunoblot analysis of TCA precipitated proteins from medium supernatant with ISG15 antibody revealed SARS-CoV-2 infection stimulated extracellular release of ISG15 from infected Calu-3 cells at 120hpi (Fig. 1B). This ISG15 release corresponded with 37% cell death in infected cells at 120hpi (Fig. 1C). These results indicate that SARS-CoV-2 infection of human lung epithelial cells induced ISGylation and extracellular release of ISG15 late during infection.

Since ISGylation and ISG15 release were noted in SARS-CoV-2 infected epithelial cells (Fig. 1A, B), we next examined whether viral encoded factor(s) could be responsible for such activity. We focused on the role of the SARS-CoV-2 spike (S) protein because previous reports have shown upregulation of ISG15 in cells expressing the S protein[15]. Nevertheless, it is still unknown whether SARS-CoV-2 S protein can trigger ISGylation and ISG15 release. We expressed human coronavirus S proteins tagged with C9 peptide in human lung epithelial A549 cells. A549 cells were transfected with the plasmids for 24h and were then washed and incubated with fresh plasmid-free medium for an additional 16 and 24 hours prior to collection of cell lysates for

immunoblotting (Fig. 1D). In contrast to empty control plasmid, ectopic expression of the SARS-CoV-2 (SARS2) S protein promoted expression of intracellular ISG15 and ISGylation in A549 cells (Fig. 1E, left panel). As a positive control, we also treated A549 cells with IFN- β, a potent ISGylation inducer[21] (Fig. 1E, right panel). Expression of C9 peptide tagged S proteins from the human coronaviruses SARS-CoV-1 (SARS1), Middle East Respiratory Syndrome coronavirus (MERS) and 229E also led to enhanced intracellular ISG15 expression and ISGylation in A549 cells (Fig. 1F), suggesting that intracellular expression of S proteins from various coronaviruses can trigger ISGylation. In contrast, A549 cells treated with purified SARS-CoV-2 S protein (full length or the S1 subunit) failed to induce ISG15 expression or ISGylation (Supp. Fig. 1A). Thus, S protein expression in coronavirus infected epithelial cells may represent a common mechanism driving ISGylation, which we show occurring during late infection of SARS-CoV-2 infected epithelial cells, after PLpro was no longer detected (Fig. 1A).

We next evaluated whether the S protein can also promote extracellular release of unconjugated ISG15. Cells expressing the SARS-CoV-2 (SARS2) S protein released ISG15 into the medium as shown by immunoblotting of TCA precipitated medium supernatant with ISG15 antibody (Fig. 1H). Thus, the S protein of SARS-CoV-2 is a viral factor that not only triggers expression of ISG15 and ISGylation, but it also facilitates extracellular release of unconjugated ISG15.

Infection with Respiratory Syncytial virus (RSV) induces ISGylation and extracellular release of ISG15 from epithelial cells

We next investigated whether infection with respiratory syncytial virus (RSV), a respiratory RNA virus that lacks de-ISGylase (e.g, PLpro of SARS-CoV-2) activity, promotes ISGylation and release of ISG15 from epithelial cells. We infected human lung epithelial A549 cells with recombinant RSV expressing mKate2 RFP protein (mKate2-RSV). We used mKate2-RSV to monitor virus infection status by immunoblotting with RFP antibody. RSV infection induced expression of intracellular ISG15 and ISGylation within 48hpi (Fig. 2A). We also detected extracellular release of ISG15 at 48hpi (Fig. 2B). In contrast to SARS-CoV-2 (Fig. 1C), ISG15 release from RSV infected A549 cells occurred independent of lytic cell death since cell death at 48hpi was negligible (i.e., less than 3% cell death) (Fig. 2C). Although ISGylation has been noted in RSV infected cells by us (Fig. 1A) and other studies[16,17], ISG15 release from RSV

infected cells had not been reported. Our results show that RSV is another respiratory RNA virus that mediates the extracellular release of ISG15 during infection.

Extracellular ISG15 induces intracellular ISG15 levels and ISGylation: upregulation of intracellular ISG15 protein in uninfected bystander cells during virus infection

Two clinically important human pathogens, SARS-CoV-2 and RSV triggered extracellular release of ISG15 from lung epithelial cells during infection (Fig. 1B, 1H, 2B). To dissect the role of extracellular ISG15, we used purified recombinant ISG15 protein (rISG15) (Supp. Fig. 1B) to investigate whether extracellular ISG15 can induce intracellular ISG15 protein levels and ISGylation in uninfected cells. Treatment of two human lung epithelial cell lines, A549 (Fig. 3A) and Calu-3 (Fig. 3B), with purified rISG15 led to induction of intracellular ISG15 and ISGylation in both cell types as early as 6 hours post-treatment as deduced by western blotting with ISG15 antibody. This result suggests that extracellular ISG15 may enhance the pool of intracellular ISG15 protein levels to upregulate ISGylation activity in uninfected cells. It is important to note that ISG15 detected in the blot constitutes intracellular ISG15 protein since we detected ISG15 in cell lysate collected after trypsin treatment (to remove extracellular rISG15) of rISG15 incubated cells. Additionally, western blotting (with avidin antibody) of trypsin treated cells incubated with biotinylated-ISG15 (biot-ISG15) failed to detect biot-ISG15 (data not shown), which demonstrated that extracellularly added ISG15 is not internalized, and that we are specifically detecting intracellular levels of ISG15 protein.

Since virus infection resulted in the extracellular release of ISG15 (Fig. 1B and 2B) and extracellular ISG15 triggered intracellular ISG15 protein induction (and ISGylation) (Fig. 3A, B) we postulate that ISG15 released from virus infected cells may act via paracrine action on uninfected bystander cells to promote ISG15 induction in those cells. To mimic this scenario, we infected A549 cells with mKate2-RSV at low MOI (MOI = 0.1) to ease the distinction between infected and uninfected cells. Fixed cells labelled with ISG15 antibody and FITC were subjected to fluorescence microscopy to detect infected cells (red-positive for mKate2) and uninfected cells expressing ISG15 (green cells). Interestingly, we visualized robust expression of ISG15 in uninfected bystander cells (Fig. 3C). This result suggested that during virus infection uninfected bystander cells undergo priming for expression of ISG15 protein and this priming may be

mediated by extracellularly released ISG15 from virus infected cells since extracellular ISG15 induces ISG15 expression in uninfected cells (Fig. 3A, 3B).

While extracellular ISG15 has a cytokine-like activity in immune cells,[6,8,18,19] our study highlights a previously unknown pro-ISGylation activity of extracellular ISG15. Our results show that extracellular ISG15 can upregulate intracellular ISG15 protein levels and ISGylation in uninfected cells (Fig. 3A, B). Indeed, our fluorescent microscopy result (Fig. 3C) suggested a probable paracrine activity of extracellular ISG15 during virus infection as uninfected bystander cells displayed expression of intracellular ISG15 protein. As intracellular ISG15 and ISGylation participate in innate antiviral defense[2], we envision a paracrine antiviral function of extracellular ISG15 released from infected cells in priming or pre-activating the host defense apparatus in uninfected bystander cells prior to infection. Likewise, extracellular ISG15 may act on virus infected cells via an autocrine mechanism to amplify ISG15 expression and ISGylation in infected cells for optimal ISGylation-dependent antiviral response.

Extracellular ISG15 induces intracellular ISG15 protein and ISGylation in target cells via a type-I interferon-independent mechanism

Purified ISG15 protein rapidly and robustly induced intracellular ISG15 levels and ISGylation after exogenous addition to epithelial cells (Fig. 3A, 3B). These findings are intriguing because Interferon Stimulated Genes like ISG15 are typically linked to type-I interferon (IFN) response[6,14]. ISG15 was expressed in uninfected bystander cells near RSV-infected cells (Fig. 3C), which could be a result of IFN signaling. Therefore, we investigated whether the ISGylation activity of extracellular ISG15 is mediated via an IFN-dependent mechanism.

Wild-type 2fTGH cells and their counterpart U5A cells, which lack a functional type-I interferon (IFN) receptor (IFNAR), were used to probe the involvement of IFN during extracellular ISG15 mediated response. As expected, in contrast to wild-type 2fTGH control cells, U5A cells lacked ISGylation and expression of intracellular ISG15 following treatment with IFN-β (Supp. Fig. 2A). In contrast, both 2fTGH and U5A cells displayed robust induction of intracellular ISG15 and ISGylation following treatment with purified ISG15 protein (rISG15) (Fig. 4A). This unexpected result was further validated using VeroE6 epithelial cells which do not produce IFN.

Like U5A cells, treatment of IFN incompetent VeroE6 cells with rISG15 protein led to rapid and robust induction of intracellular ISG15 protein and ISGylation (Fig. 4B). These results together demonstrate that extracellular ISG15-mediated induction of intracellular ISG15 and ISGylation occurs through an IFN-independent mechanism.

Next, we evaluated whether viral infection could induce intracellular ISG15 protein and ISGylation in IFN-deficient VeroE6 cells. RSV infection robustly induced intracellular ISG15 and ISGylation in VeroE6 cells (Fig. 4C). Additionally, RSV infected VeroE6 cells were competent in extracellular release of ISG15 protein (Fig. 4D). As with infected A549 cells (Fig. 2C), the release of ISG15 from infected VeroE6 cells was independent of lytic cell death since cell death was not observed during the same time-frame as ISG15 release (Supp. Fig. 2B). Since RSV infected VeroE6 cells released ISG15 during infection, we examined the status of ISG15 in uninfected VeroE6 cells during RSV infection. As with IFN-competent A549 cells (Fig. 3C), we infected IFN-deficient VeroE6 cells with mKate2-RSV at low MOI (MOI = 0.1) followed by fluorescence microscopy to detect infected cells (red cells – positive for mKate2) and cells expressing ISG15 (green cells – labelled with ISG15 antibody and FITC). We visualized ISG15 protein both in uninfected and infected VeroE6 cells (Fig. 4E). Our immunofluorescent studies with VeroE6 cells show IFN independent induction of intracellular ISG15 protein in uninfected bystander cells, potentially via paracrine action of extracellular ISG15 released from virus infected cells. Thus, we have identified a yet unknown activity of extracellular ISG15 protein in triggering ISG15 expression and ISGylation, which unexpectedly occurred via an IFN-independent mechanism. To the best of our knowledge, this is the first report of an IFN-independent mechanism for intracellular ISG15 expression and ISGylation during virus infection.

IFN-independent antiviral activity of extracellular ISG15

Extracellular ISG15-mediated induction of intracellular ISG15 protein and ISGylation via an IFN-independent mechanism (Fig. 4) prompted us to explore its implications during virus infection. RSV infection triggered ISG15 release, and ISG15 protein levels were induced in bystander uninfected cells (Fig. 2 and Fig. 4). Therefore, we postulated that extracellular ISG15 may possess an innate host defense function that can limit virus infection.

To evaluate the antiviral activity of extracellular ISG15, we pre-treated human lung epithelial A549 cells with purified ISG15 protein (rISG15), followed by RSV infection. Extracellular ISG15 mediated restriction of RSV infectivity and spread was evident in phase-contrast microscopy showing reduced cytopathic effect (CPE) following rISG15 treatment versus extensive CPE in vehicle treated infected A549 cells (Supp. Fig. 3A). This result was confirmed by observing diminished virus replication in mKate2-RSV infected A549 cells treated with rISG15 (Supp. Fig. 3B). Most importantly, plaque assay analysis for infectious viral titer revealed loss of infectivity (reduction by one log or 10- fold) following extracellular rISG15 treatment of RSV infected A549 cells (Supp. Fig. 3C). Accordingly, a representative plaque assay for infectious viral titer also showed drastic reduction in plaques from rISG15 treated infected A549 cells compared to control vehicle treated infected cells (Supp. Fig. 3D). These results demonstrated antiviral activity of soluble extracellular ISG15.

Identification of extracellular ISG15 as an antiviral factor prompted us to investigate whether such antiviral activity is mediated by the IFN response. For our studies we used IFN-incompetent VeroE6 cells since they do not produce IFN and thus lack IFN-dependent responses. RSV infection in VeroE6 cells treated with rISG15 was analyzed using the same methods as described above for IFN-competentA549 cells. Although VeroE6 cells lack IFN signaling, extracellular ISG15 still conferred protection against virus infection as inferred from – a) diminished viral replication as deduced from loss of mKate2 expression in mKate2-RSV infected VeroE6 cells treated with rISG15 (Fig. 5A), b) reduced virus-associated CPE in rISG15 treated cells (Fig. 5B), and c) plaque assay result showing reduced infectious viral titer due to rISG15 treatment (Fig. 5C and Supp. Fig. 3E). Viral infectivity was significantly reduced by more than 10-fold following treatment of VeroE6 cells with rISG15 (Fig. 5C). Thus, we have identified extracellular ISG15 as a new soluble antiviral factor which operates via IFN-independent mechanism.

RSV does not encode de-ISGylases such as PLpro of SARS-CoV-2. Therefore, in contrast to RSV, treatment of Calu-3 and VeroE6 cells with extracellular ISG15 failed to alter SARS-CoV-2 replication (Supp. Fig. 4A, 4B). Since ISGylation confers antiviral activity, we postulate that de-ISGylase activity of PLpro prevents extracellular ISG15 mediated ISGylation-dependent antiviral responses against SARS-CoV-2.

Viruses trigger ISG15 release, and we now show that extracellular ISG15 possesses antiviral activity. Like IFNs, extracellular ISG15 may restrict virus spreading by priming uninfected bystander cells into an antiviral state to ensure reduced viral replication following subsequent infection. Therefore, we next investigated whether extracellular ISG15 released from infected cells is involved in restricting virus infection and spread. To assess the function of endogenously released extracellular ISG15 during virus infection, we blocked the ISGylation activity of extracellular ISG15 with an anti-ISG15 polyclonal antibody. Addition of ISG15 antibody, but not IgG isotype control, drastically reduced induction of intracellular ISG15 levels and ISGylation mediated by extracellular ISG15 (Supp. Fig. 5). Therefore, we used the extracellular ISG15 blocking antibody to examine the antiviral role of ISG15 released during virus infection of IFN-deficient VeroE6 cells. Plaque assay analysis revealed approximately 15-fold more infectious virus in ISG15 antibody treated cells compared to control IgG antibody treated cells (Fig. 5D). Concomitantly, blockade of endogenously released extracellular ISG15 led to enhanced mKate2-RSV infection since we detected higher levels of mKate2 in ISG15 antibody treated cells compared to control IgG treated VeroE6 cells (Fig. 5E). These results demonstrated that extracellular release of ISG15 protein during virus infection confers robust IFN-independent antiviral activity. Thus, we have uncovered extracellular ISG15 as a novel soluble antiviral factor that is released during virus infection as a component of host defense apparatus to ensure reduced viral infection and spread.

Extracellular ISG15 induces intracellular ISG15 for ISGylation via integrin-FAK pathway: interaction of ISG15 with α5β1 integrin

To elucidate the mechanism by which extracellular ISG15 mediates IFN-independent ISGylation, we aimed to identify cell surface molecules that engage with extracellular ISG15. We conducted a preliminary mass spectrometry experiment to identify potential cell surface molecules interacting with extracellular ISG15. For this experiment, we biotinylated purified ISG15 protein (Biotinylated-ISG15). Chilled human lung epithelial A549 cells were incubated with biotinylated-ISG15 at 4°C to prevent internalization of extracellular ISG15. The cell lysate was then precipitated with avidin-agarose, and the bound proteins were subjected to mass spectrometry. Mass spectrometry analysis revealed the interaction of extracellular biotinylated-ISG15 with various cell surface molecules of A549 epithelial cells, including the β1integrin (data

not shown). A previous study has shown extracellular ISG15 interacting with integrin molecule LFA-1 in immune cells[8]. Given that LFA-1 is expressed only in immune cells and is not expressed in non-myeloid epithelial cells like A549, we chose β1 integrin for further analysis since, like LFA-1, it belongs to the integrin family of proteins. Because cell surface integrins are signaling receptors that activate the integrin-FAK pathway, we focused our studies on the possibility of extracellular ISG15 interacting with integrin to activate FAK signaling, resulting in IFN-independent ISGylation.

Functional integrin molecules exist as heterodimers of α and β subunits[21,22,23]. Our mass spectrometry analysis identified β1 integrin as a putative extracellular ISG15 interacting factor and therefore, we investigated whether α5β1 integrin interacts with extracellular ISG15. We confirmed the interaction of extracellular ISG15 with the α5β1 integrin by incubating chilled A549 cells with purified ISG15 protein at 4ºC, followed by immunoprecipitation of ISG15 bound proteins with ISG15 antibody and western blotting with α5 integrin antibody. Co-immunoprecipitation assay revealed interaction of extracellular ISG15 with α5 integrin (Fig. 6A). To investigate whether ISG15 interacts directly with α5β1 integrin we biotinylated purified α5β1integrin protein. A cell free *in vitro* interaction assay was performed by incubating purified ISG15 protein with biotinylated α5β1integrin (Fig. 6B). We incubated the purified proteins at 4ºC, followed by immunoprecipitation with avidin-agarose beads, and immunoblotting with ISG15 antibody. Our cell-free assay demonstrated direct binding of ISG15 protein with α5β1 integrin (Fig. 6B).

Activation of cell surface integrins results in transmission of downstream cellular signaling events[22,24,25,26]. To elucidate the downstream signaling pathway linked to ISG15-integrin interaction, we investigated the activation status of focal adhesion kinases (FAK)[27]. FAKs are critical cytosolic adaptors that associate with integrins to mediate signaling following its activation by phosphorylation[27]. Therefore, we examined whether outside-in activation of surface integrins by extracellular ISG15 results in phosphorylation and activation of FAK. Treatment of A549 cells with purified ISG15 protein (rISG15) indeed led to phosphorylation of FAK as detected by western blot analyses with phospho-FAK antibody (Fig. 6C). This result suggested the possibility of integrin-FAK dependent activity of extracellular ISG15. The role of the

integrin-FAK pathway in extracellular ISG15 mediated activity was assessed by using a FAK inhibitor (FAKi). Profound reduction of intracellular ISG15 protein levels (Fig. 6D) and ISGylation (Fig. 6E) was observed in A549 cells treated with rISG15 protein in the presence of the FAKi. FAKi treatment of IFN-signaling incompetent U5A cells also resulted in reduced intracellular ISG15 protein levels and ISGylation following rISG15 treatment (Supp. Fig. 6A, B), indicating that FAK is involved in extracellular ISG15 mediated response in IFN-pathway deficient cells. These results show that the integrin-FAK pathway is a signaling component of IFN-independent ISGylation mediated by extracellular ISG15.

To corroborate the role of integrin signaling during extracellular ISG15 mediated response, we next utilized α5 integrin knockout (ITGA5 KO) human HAP1 cells generated by CRISPR-Cas9 technology[28,29]. Compared to wild-type HAP1 cells, treatment of α5 integrin KO cells with rISG15 led to diminished intracellular ISG15 protein levels and ISGylation (Fig. 6F), confirming the role of integrin during extracellular ISG15 mediated response. We further validated these results using an RGD (Arginine- Glycine-Aspartic acid or Arg-Gly-Asp) peptide to block ligand-integrin interaction. Extracellular matrix (ECM) proteins (e.g., fibronectin, vitronectin, fibrinogen, and von Willebrand factor) utilize the RGD motif to interact with cell surface integrins. Thus, RGD peptides can block the integrin ligand binding site and impair interactions with extracellular ECM ligands and subsequent downstream signaling[30–33]. To determine whether extracellular ISG15 also interacts with integrins similar to RGD-motif containing ECM proteins, we treated A549 cells with rISG15 in the presence of either a control peptide or RGD peptide. RGD peptide treatment resulted in reduced extracellular ISG15 dependent ISGylation (Fig. 6G) and intracellular ISG15 (Fig. 6H). RGD peptide also reduced extracellular ISG15 dependent induction of intracellular ISG15 protein and ISGylation in IFN-incompetent U5A cells, confirming that this mechanism is IFN-independent (Supp. Fig. 6C). This study shows that ISG15 interacts with integrins like other RGD-motif containing integrin ligands. Our *in silico* molecular modeling studies described below provide additional mechanistic insights on ISG15-integrin interaction via RGD-like motifs in ISG15 protein (Fig. 7).

Molecular modeling of extracellular ISG15-α5β1 integrin interaction

Integrin receptors are composed of two types of transmembrane subunits, α and β, forming heterodimeric molecules. Through various combinations of α and β subunits, integrins exhibit multiple subtypes and diverse ligand specificity, enabling them to interact with different ECM molecules[34]. α5β1 integrin preferentially binds to and is activated by ECM ligands containing the RGD motif, such as fibronectin (Fig. 7A, 7B)[35]. The RGD motif of fibronectin binds within the cleft formed at the interface of the α5 and β1 subunits of integrin. The arginine (Arg) of the RGD motif binds to the α5 subunit, while the aspartic acid (Asp) binds to the β1 subunit, thereby bridging the α-β subunits of integrin (Fig. 7B). Earlier studies on RGD-binding integrins reported that specific structural changes associated with receptor activation occur only in the β subunit of integrins, and that the presence of the aspartic acid within the RGD motif alone is sufficient to activate the receptor[36,35]. Additionally, a recent cryo-EM structure report showed that instead of aspartic acid (Asp), integrin α6β1 recognizes ECM ligand laminin through a glutamic acid (Glu) residue that binds to the β1 subunit of the integrin receptor[37].

Based on this evidence, we analyzed surface-exposed Arg-Asp and Arg-Glu residue combinations on ISG15 as the potential integrin binding hotspots. ISG15 is comprised of two Ubiquitin-like β-grasp domains (Fig. 7C)[38]. Within this domain, ISG15 has five different sites with exposed Arg-Asp/Glu residue combinations on its surface (Supp. Figure 7). Each of these five sites of ISG15 was docked individually with the RGD binding site of integrin α5β1 for analysis of activation-specific interactions. Among the docked sites, Site-3 (Supp. Figure 7) comprised of the residues Arg99 (R99), Glu97 (E97), Asp79 (D79), and Glu80 (E80) exhibited interactions like the known RGD ligands of integrins such as fibronectin (Fig. 7D and 7E). The optimal binding orientation of ISG15 (Site-3) has a HADDOCK docking score of -165.6, which is higher than the scores observed for the other sites of ISG15 (Supp. Table S1). Surprisingly, we observed Glu80 binding to the aspartic acid (Asp) binding groove of the integrin rather than the typical aspartic acid residues (Fig. 7F). Our analysis revealed that ISG15-α5β1 complex is formed by an RGD-like motif in ISG15, wherein the arginine site of the RGD motif of ISG15 is occupied by Arg99 and the aspartic acid site is occupied by Glu80. Thus, our analysis has uncovered a new “non-classical” RGD-like motif in ISG15 that can be utilized to achieve similar

conformation-driven interaction with integrin similar to ECM ligands harboring “classical” RGD motif.

To further examine the stability of the ISG15- α5β1 interaction, we performed molecular dynamics (MD) simulations of the complex for 300 ns (Fig. 7G). Overall, the ISG15-integrin α5β1 complex remained stable throughout the simulation time (Fig. 7G). We also analyzed the stability of the specific interactions that reflect the RGD motif interactions. As it applies to ISG15 – integrin α5β1 complex, Glu80 in the aspartic acid binding groove formed a hydrogen bond interaction with Ser134 of α5β1. The distance between the Glu80 of ISG15 and Ser134 of α5β1 interaction initially starts below 3 Å and remained stable for 80 ns, and it shows a gradual increase in distance over time, stabilizing at around 6 Å. Conversely, the interaction between Arg99 of ISG15 and Asp227 of α5β1 shows more variation in distance, oscillating between approximately 3 Å and 10 Å over the simulation period. The Arg99 interaction may be transient and weaker, with the bond forming and breaking throughout the simulation. Upon comparison of the interactions involving Arg99 and Glu80 with the integrin, it appears that ISG15 may interact and activate integrin α5β1 through the stable interaction mediated by Glu80.

Our studies have provided novel insights on innate immune host-defense mechanism by identifying extracellular ISG15 as a new soluble antiviral factor and delineating an unexpected type-I IFN independent mechanism for ISG15 antiviral activity. We now show interaction of extracellular ISG15 with cell surface integrins activating integrin-FAK pathway to mediate IFN-independent ISGylation. Thus, we put forward a yet unknown mechanism that disengages the widely held dogma about ISGylation being invariably linked with type-I IFN response.

Discussion

Type-I IFNs are well established antiviral cytokines that confer an antiviral state by activating the JAK-STAT pathway. One of the mechanisms by which IFNs trigger antiviral response is by promoting ISGylation by inducing expression of IFN stimulated gene 15 (ISG15) protein. ISGylation is an antiviral, post-translational modification wherein intracellular ISG15 is conjugated to target proteins by enzymes related to the ubiquitination process. Although ISGylation is canonically dependent on IFN, our study reports a non-canonical IFN-independent mechanism of ISGylation. We show that extracellular ISG15 activates the integrin-FAK pathway to induce IFN-independent expression of intracellular ISG15 and ISGylation. Furthermore, we have identified extracellular ISG15 as a new soluble antiviral factor restricting virus infection via IFN-independent mechanism. Thus, our study highlights a novel mechanism of IFN-independent ISGylation linked to antiviral activity and mediated by extracellular ISG15 released from virus infected cells.

Previous studies have reported release of ISG15 from macrophages infected with SARS-CoV-2 and influenza A virus (IAV)[11]. Bronchial epithelial cells infected with rhinovirus also released ISG15 into the extracellular milieu[12]. Extracellular ISG15 did not reduce rhinovirus infection, but instead downregulated the immune response by inhibiting the release of the chemokine CXCL10 from infected cells[12]. Circulating ISG15 has been detected in serum of patients infected with SARS-CoV-2[10], and levels of free ISG15 in the saliva and nasal secretion of rhinovirus patients correlated with viral load[12]. Although extracellular ISG15 has been detected in clinical samples of virus-infected patients, the functional role of extracellular ISG15 during virus infection has not been reported, and the role of viral encoded factor(s) in ISG15 release is unknown. Previous reports have identified the SARS-CoV-2 S protein in upregulating the expression of *isg15*[15]. Our study has now identified the S protein of SARS-CoV-2 and other coronaviruses as a viral factor involved in induction of ISGylation and in ISG15 release. SARS-CoV-2 encodes a de-ISGylase (PLpro) that removes conjugated ISG15 from its targets, negating the antiviral effects of ISGylation[10,39,40]. Therefore, ISGylation has yet to be detected in SARS-CoV-2 infected cells. Although ISGylation was not observed during early- mid infection, we surprisingly detected ISGylation and release of ISG15 from SARS-CoV-2 infected human lung epithelial cells during late infection. We further show that SARS-CoV-2 PLpro expression in

lung epithelial cells during early- mid infection correlated with lack of ISGylation. However, PLpro declined during late infection, when ISGylation and ISG15 release were evident. Due to the de-ISGylase activity of PLpro, extracellular ISG15 mediated ISGylation did not reduce SARS-CoV-2 replication. Based on the activity of extracellular ISG15 on Natural Killer cells (NK cells)[8], it is possible that ISG15 released from infected epithelial cells during SARS-CoV-2 infection acts on immune cells like macrophages to shape inflammatory and adaptive responses. Indeed, it has been speculated that ISG15 release during SARS-CoV-2 contributes to hyperinflammation via uncharacterized mechanisms[41]. On the other hand, RSV does not encode a de-ISGylase, and ISGylation is effective at limiting RSV infection[16]. We now show a direct effect of extracellular ISG15 in promoting the antiviral response in epithelial cells by restricting RSV infection. Extracellular ISG15 released during RSV infection induced ISGylation in an IFN-independent manner (Fig. 3) to promote an antiviral response, which reduced RSV infection (Fig. 4 and 5). While SARS-CoV-2 triggered ISG15 release, extracellular ISG15 failed to restrict SARS-CoV-2 infection (Supp. Fig. 4) probably due to the de-ISGylase activity of PL-pro. We postulate that antiviral activity of circulating ISG15 in the extracellular milieu may dictate disease outcome and secondary complications during virus infection. Therefore, viruses like SARS-CoV-2 have evolved to encode viral proteins like PL-pro to antagonize the antiviral effect of extracellular ISG15 by blocking ISGylation. In contrast, ISGylation mediated antiviral activity by extracellular ISG15 cannot be counteracted by viruses like RSV that do not possess any viral tools to antagonize ISGylation.

ISG15 release has also been documented in non-viral settings, including treatment of myeloid cells (NK cells, PBMCs, T-cells) with various pathogen associated molecular patterns (PAMPs) and over-expression of ISG15 in HEK293 cells[7]. Extracellular ISG15 released from HEK293 cells interacted with LFA-1 integrins on NK cells and induced the release of IFNγ, but only when paired with IL-12[8]. Contrasting these studies, we show that extracellular ISG15 alone elicited expression of ISG15, ISGylation, and antiviral response in epithelial cells. Our data and that in myeloid cells highlights cell-dependent immunomodulatory activities by extracellular ISG15 dictated by its interaction with two unrelated cell surface integrins: LFA-1 in myeloid cells[8] and α5β1 in non-myeloid epithelial cells (our study).

In immune myeloid cells, extracellular ISG15 interacts with the integrin LFA-1 and signals through intracellular Src proteins, leading to the release of IFNγ[8] in IL-12 primed NK cells[19,42]. We have identified pro-ISGylation and anti-viral activity of extracellular ISG15 in non-myeloid epithelial cells. However, LFA-1 is only expressed in myeloid cells[43], and thus the receptor involved in transducing the activity of extracellular ISG15 in non-myeloid cells was unidentified. Although epithelial cells do not express LFA-1, other integrins are expressed at their surface. Among the pool of epithelial surface integrins, α5β1 integrins are highly abundant in lung tissue. α5β1 integrins are involved in tissue remodeling and respiratory diseases[44] like asthma[45], pulmonary fibrosis[46], and cystic fibrosis[47]. α5β1 integrins participate in cell survival and adhesion by binding to RGD (Arginine, Glycine, Aspartic Acid) motif containing proteins like fibronectin within the extracellular matrix (ECM). To do this, α5β1 integrin adopts a half-bent conformation. This leaves its RGD binding domain partially exposed to interact with RGD containing ECM proteins[48]. Like other integrin ligands, ISG15 has an RGD-like domain (Fig. 6) that facilitates interaction with α5β1 to trigger outside-in signaling[49]. Our *in silico* molecular docking studies show that ISG15 can interact with the RGD binding region of α5β1 by utilizing Arginine and Glutamic acid amino acids to mimic the Arginine and Aspartic acid residues of the RGD motif. Indeed, extracellular ISG15 interacted with α5β1 integrin in a cell free interaction assay and with the epithelial cell surface α5β1 integrin. This type of interaction is similar to that between extracellular ISG15 and LFA-1[8]. ISG15/LFA-1 interaction culminated in IFNγ production from myeloid cells, while our study demonstrated ISG15/ α5β1 integrin interaction leading to intracellular ISGylation independent of the canonical IFN-dependent mechanism.

FAKs are the main mediators of integrin signaling[48]. Ligands bind to integrins which rearrange into focal adhesions, leading to activation of submembrane FAK molecules by its autophosphorylation[49]. For example, fibronectin, which has an RGD domain, can bind to integrins and activate STAT1 in a mechanism dependent on activated FAK[50]. FAK also forms complexes with downstream adapters, like Src, to continue a phosphorylation cascade to activate other proteins[56,57]. We show FAK activation by extracellular ISG15 (Fig. 6). In addition, when FAKs are chemically blocked prior to extracellular ISG15 treatment, ISGylation is impaired (Fig. 6), suggesting that the integrin-FAK cascade is involved in extracellular ISG15 mediated ISGylation. FAKs also play a role during virus infection to activate proteins that are associated

with different stages of the innate immune response. MAVS- mediated antiviral signaling was shown to be facilitated by FAK localization to the mitochondrial membrane during Sendai Virus (SeV) infection[51]. Phosphatidylinositol 3-kinase (P13K) signaling during influenza A virus (IAV) infection was also found to be regulated by FAK phosphorylation[52]. Thus, FAK participation in ISG15-integrin signaling in promoting an antiviral response is to be considered in future studies.

Other studies have also shown that ISGs can be induced independent of IFN. Several ISGs, including IFIT1, IFIT2, IFIT3, Mx1, Mx2, CXCL10, and ISG15 were upregulated transcriptionally following human cytomegalovirus (HCMV) infection independently of type-I IFN[53]. This effect was reported to be dependent on IRF3 activation by an unknown mechanism[53]. Presumably, IFN-independent ISG15 induction may occur during HCMV infection via virus encoded factor including dsDNA mediated activation of the STING pathway[54]. Transcription factor IRF7 can also induce ISGs (i.e., ISG15) independent of IFNs by binding to the interferon stimulated response element (ISRE)[55]. Additionally, bacteria such as *Listeria* and *Mycobacterium* can induce ISG15 gene expression via IFN-independent cytosolic surveillance pathway (CSP). This pathway induces ISG15 mRNA expression after sensing bacterial DNA[56]. These reports identify intracellular factors that can induce ISG15 independent of IFN. Unlike these studies, our report is novel in that it identifies a function of extracellular ISG15 as an outside-in signal to induce ISGylation in uninfected cells, bypassing the need for intracellular PAMPs (such as dsDNA, bacterial DNA) or extracellular IFN to initiate this response. Furthermore, IRF7 expression is limited to hematopoietic cells, whereas our studies were conducted with non-hematopoietic epithelial cells[57,58]. Our study also identifies a receptor for ISG15 on epithelial cells and identifies upstream signaling via α5β1 integrins and FAK to modulate paracrine ISG15 IFN-independent activities.

Extracellular ISG15 may not only bind to α5β1, but a diverse set of integrins on the surface of multiple cell types that in turn may govern additional facets of antiviral activity. Viruses such as Ebola virus[59], Epstein Barr virus[60], and foot and mouth disease virus can use α5β1 and other integrins for cellular entry. Extracellular ISG15 may block virus entry by occupying or altering the conformation of integrins to prevent virus from interacting efficiently with integrin receptors

for cellular entry. This is an intriguing research avenue for the development of ISG15 derived competitive virus inhibitors and therapeutics or to prevent off-site effects from extracellular ISG15 at distant sites. In summary (Fig. 8), our studies identified ISG15 as a new extracellular antiviral factor that triggers ISGylation in an IFN-independent mechanism. Here, extracellular ISG15 interacts with cell surface integrins to trigger FAK-dependent ISGylation. Since ISGylation occurs widely during virus infection, this mechanism has broad implications for understanding virus-host interactions and development of host-directed therapeutics against multiple viruses.

Authorship

L.G.M, K.C, C.M, I.M, S.P, L.M, and T.A.M. performed the experiments. L.G.M, K.C, C.M, A.L.H, S.N, T.A.M, S.B contributed to the experimental design, data analyses and interpretation, L.G.M, K.C, C.M prepared the figures and tables, manuscript was written by L.G.M, K.C, C.M, S.N, T.A.M, S.B.

Acknowledgements & Funding

This research was supported by funding from the Washington Research Foundation (SB), National Institutes of Health (NIH) R01AI083387 (SB), and R01GM137022 (SN). LGM was supported by NIH NIGMS Predoctoral Biotechnology Training Grant 5T32GM008336. Biorender was used to create the model and timelines for this project.

Conflict of Interest Disclosure: Authors have no conflict of interest to declare.

Materials and Methods

Cell Culture: A549, Calu-3, and VeroE6 cells were maintained in DMEM (GIBCO #11995065) supplemented with 10% FBS, 100 IU/ml penicillin, and 100 g/ml streptomycin. CV-1, U5A and 2FTGH cells were maintained in DMEM supplemented with 5% FBS, 100 IU/ml penicillin, and 100 g/ml streptomycin. HAP1 and ITGA5 KO cells were maintained in IMEM supplemented with 10% FBS and 100 IU/ml penicillin, and 100 g/ml streptomycin.

Cell Transfection: pcDNA3.1 plasmids encoding the C9- tagged SARS-CoV-2 S protein (pcDNA3.1-SARS2-S) (Addgene plasmid # 145032)[62], SARS-CoV S protein, MERS S protein, HCoV- 229E S protein were used in these experiments; all were provided by Dr. T. Gallagher (Loyola University Chicago). Cells were transfected with C9-tagged SARS-CoV-2 S protein or with empty vector (pcDNA3.1) using Lipofectamine 2000 (Invitrogen) and maintained in antibiotic free DMEM supplemented with 10% FBS. After 24 hours, the media was changed and the WCL or supernatant was collected at the indicated timepoints.

Recombinant S protein, IFN-β, ISG15, FAK inhibitor (FAKi), and RGD Blocking Peptide Treatment: Cells were treated with 500 U/ml of IFN-β (Sino Biological, catalog no. 10704-HNAS) or vehicle prepared in antibiotic free DMEM supplemented with 10% FBS. A549, VeroE6, U5A, 2FTGH, HAP1, and ITGA5 KO cells were also treated with 5µg/mL of recombinant purified ISG15 (Sinobiological, catalog no.12729 -HNAE1) for indicated times before collection of whole cell lysates. For FAK inhibitor experiments, A549 and U5A cells were treated with the FAK inhibitor (PF-431396 hydrate; Sigma -Aldrich, catalog no. PZ0185) at a concentration of 20µM in 10% or 5% antibiotic- free media, respectively. After 2 hours, 1µg/mL of rISG15 was added to the media containing FAKi. Alternatively, A549 cells were pretreated for 2 hours using 200µM of RGD (AnaSpec Inc., catalog no. AS-62049) blocking peptide or control peptide (Enzo, catalog no. BML-P7-1-0005) before adding 2µg/ml rISG15 to the media for 4 hours. In some experiments, A549 cells were treated with 8nM of full-length SARS-CoV-2 S protein (BEI catalog no. NR-52397) or the S1 subunit (SinoBiological, catalog no. 40591- V08HB) for 16 hours before collection of whole cell lysate.

Immunoblot: Whole cell lysates (WCL) were collected using 1x Laemmli sample buffer containing beta-mercaptoethanol. Lysates were subject to gel electrophoresis in an acrylamide gel and then transferred to Amersham Protran 0.2-um nitrocellulose blotting membranes. Membranes were blocked in 5% milk with PBS-T for 5 hours at room temperature and blotted with primary antibodies against ISG15 generated as described previously[63], Rhodopsin C9 (Invitrogen, catalog no. MA1-722), S1 (Sinobiological), RFP (ThermoFisher Scientific, catalog no. MA5-15257), pFAK(Y397) (Cell signaling, catalog no. 8556P), FAK (Cell signaling catalog no. 13009S), a5 integrin (Proteintech Catalog no.10569-1-AP), and actin (Bethyl Laboratories, Inc., catalog no. A300-491A) overnight at 4°C. Secondary antibodies conjugated to horseradish peroxidase were added for 1.5 hours at room temperature. Protein bands were developed using Western Lightning Plus-ECL (Perkin Elmer catalog no. 104001EA) visualized and quantified using ChemiDoc XRS software Image Lab 5.1 (Bio-Rad).

RNA Extraction and RT-qPCR: RNA was extracted using Trizol reagent (Life Technologies, catalog no. 15596026) following the manufacturer's instructions. RNA was treated with ezDNase and cDNA was synthesized using SuperScript IV VILO Master Mix (Thermo Fisher, catalog no. 11766050). qPCR was performed using PowerUp SYBR Green Master Mix following manufacturer's instructions (Thermo Fisher; catalog no.A25741) qPCR was performed in a StepOnePlus Real-Time PCR System (Applied Biosystems). Abundance of SARS-CoV-2 N mRNA was normalized to that of GAPDH. The following primers were used:

SARS-CoV-2 N	Fw: 5′-CAATGCTGCAATCGTGCTAC-3′
	Rv: 5′-GTTGCGACTACGTGATGAGG-3′
GAPDH	Fw: 5'- ACAACTTTGGTATCGTGGAAG-3'
	Rv: 5'- GCCATCACGCCACAGTTTC-3'

TCA Precipitation of Proteins from Cell Culture Medium: A549 cells were transfected with S protein or pcDNA3.1 at 1µg/ml for 24 hours. Media was changed to remove plasmids and cells were cultured for an additional 16 or 24 hours. Plasmid-free cell culture supernatants were collected and clarified to remove cell debris. Total proteins in culture supernatants were precipitated with Trichloroacetic acid (TCA, 20% v/v final concentration) overnight at 4°C.

Protein pellets were washed three times with 200ul of ice-cold acetone. Pellets were resuspended in 2X Laemmli buffer with b-mercaptoethanol and neutralized with 1M Tris-HCL at pH 8.0 before immunoblotting with indicated antibodies.

Viruses: SARS-CoV-2 isolate USA-WA1/2020 (BEI resources catalog no. NR-52281) was propagated in VeroE6 cells. SARS-CoV-2 and mock containing cell lysate stocks were generated. Human respiratory syncytial virus A2 strain was purified using previous methods[64–67]. Recombinant RSV expressing mkate2 (RSV-mkate2) was propagated as described previously[68].

Infection Experiments: Work with infectious SARS-CoV-2 was performed in biosafety cabinets within a biosafety containment level 3 facility at Washington State University. Personnel wore powered air purifying respirators during all procedures (MAXAIR Systems, Irvine, CA). Calu-3 cells were seeded and incubated for 48 hours before SARS-CoV-2 infection at an MOI of 0.1 or mock infection. After indicated times, culture supernatants were collected for TCA precipitation (20% v/v final concentration) followed by immunoblotting. Whole cell lysates were collected in Laemmli buffer for immunoblotting. Calu-3 and VeroE6 cells were also pretreated with 5ug/mL of ISG15 for 16 hours and then infected with SARS-CoV-2 at an MOI of 0.1 for RNA collection using Trizol. A549 and VeroE6 cells were infected with RSV-mkate2 for 48h at an MOI of 0.1. Whole cell lysate was collected in Laemmli buffer for immunoblotting and supernatants were collected for TCA precipitation assays. In some experiments, A549 and VeroE6 cells were pretreated with 5µg/mL of ISG15 for 8 hours, and then infected with either RSV-mkate2 or wt-RSV for 48 hours. Whole cell lysate of RSV-mkate2 infected samples were collected in Laemmli buffer and subject to immunoblotting. Supernatants of samples infected with non-tagged RSV were collected for plaque assay. For plaque assays, CV-1 cells were infected with ten-fold dilutions of the supernatants. After 1.5h adsorption, methyl cellulose was added to the wells, and incubated for 48-72 hours. The methyl cellulose was removed, and the plates were dyed with crystal violet in 70% ethanol. After 45 minutes, the plates were washed with ddH_2O. Vero cells were also infected with RSV-mkate2 at an MOI of 0.1 for 48h in the presence of either rabbit IgG (Cell signaling, catalog no. 2729) or IgG antibodies against ISG15. Lysate was subject to immunoblotting, and supernatant was used to perform TCID50 assays. Infectious virus titer was calculated using the Reed and Meunch method.

LDH Assays: Supernatant of mock and either RSV or SARS-CoV-2 infected samples was collected at indicated timepoints. LDH assays were performed according to manufacturer's instructions (Abcam, catalog no. AB65393). To calculate the percentage, we used the calculation: ((test sample- low control)/ (high control- low control))× 100.

Imaging: VeroE6 or A549 cells seeded on chamber slides were pretreated with 5µg/mL of ISG15 for 8 hours and then infected with RSV at an MOI of 1 for 16 hours. Live cells were imaged using a Leica microsystems microscope (Model DM18). A549 or VeroE6 cells were also infected with RSV-mkate2 at an MOI of 0.1 for 48 hours. Infected cultures were washed and fixed in paraformaldehyde 4%, blocked in 5% BSA in PBS-T and incubated overnight with primary antibodies against ISG15. Slides were incubated with labeled secondary antibodies (CoraLite488-conjugated, proteintech, catalog no. SA00013-2) and counterstained with DAPI (4µg/mL), and mounted with ProLong Gold antifade (Invitrogen, catalog no. P36930), and were also imaged using a Leica microsystems microscope (Model DM18).

Interaction Assays: For cell-free assays, purified α5β1 integrin protein (Yo proteins, catalog no. 638) was biotinylated by combining α5β1 integrin with biotin and dPBS, and crosslinking under UV light. Biotinylated α5β1integrin (5.7 mM) was then added to NeutrAvidin Agarose Resin beads (Thermoscientific, catalog no. 29200) and incubated at 4°C overnight. rISG15 was added the next day and incubated at 4°C overnight. 2X Laemmli sample buffer was added and followed by immunoblotting. For experiments with cells, A549 cells were chilled at 4°C for 15 minutes prior to treatment with 5µg/mL rISG15 for 4 hours at 4°C. The lysate was collected, and then added to ISG15 antibody bound beads overnight.

Docking of ISG15 and Integrin α5β1: For modeling the ISG15-integrin α5β1 complex, protein-protein docking was carried out. The crystal structures of ISG15 (PDB ID: 3RT3) and integrin α5β1 (PDB ID: 7NWL) were downloaded from the Protein Data Bank[70]. Missing side-chain atoms and residues were added, and the structure was optimized using the structure preparation module of MOE[71]. For the docking of ISG15 with integrin α5β1, the residues comprising the RGD motif binding site (Tyr186, Phe187, Gln189, Gln221, Ser224, and Asp227 of the α5-β propeller domain, and Ser132, Tyr133, Ser134, Gly223, Asn224, Leu225, Asn226, Ser227, and

Glu229 of the β1-βI domain) of α5β1 were selected as the potential interaction site. For ISG15, the exposed arginine and aspartic acid residues (similar to the RGD motif) were used as the possible interaction site. ISG15 has five surface-exposed combinations of arginine with aspartic acid residues. Each site of ISG15 was docked to the α5β1 integrin's RGD binding site. Protein-protein docking simulations were performed using the HADDOCK v2.4 server[72,73]. For each protein-protein docking run, at most 20,000 possible binding orientations were generated, among which 2000 poses were considered for post-docking minimization. Finally, 1,000 poses were filtered and used for scoring and clustering. Among the resulting clusters with multiple docking poses, a cluster exhibiting interactions resembling those of the RGD motif of integrins was selected for subsequent MD simulation.

MD Simulation of ISG15 - α5β1 complex: The stability of the ISG15-α5β1 complex was further examined using molecular dynamics simulations using AMBER v20[74]. The input files for the MD simulation were generated using the Input Generator-Solution Builder module of CHARMM-GUI with AMBERff14SB forcefield[75]. The system was solvated using TIP3P water molecules in a cubic box such that the distance between any atom of the protein complex and the box edge was at least 10 Å[76]. Subsequently, the system was neutralized (net charge = 0), and the salt concentration was brought to 0.15 M by adding Na+ and Cl− ions. The simulations were performed under periodic boundary conditions and with the Particle Mesh Ewald (PME) method for calculating the long-range electrostatic interactions[77,78]. The van der Waals interactions were smoothly switched off at 12 A°. Further, the solvated system was minimized (10,000 steps) to remove any steric clashes in the system. Following the minimization step, equilibration and production runs were performed with an integration time step of 2 fs, and all the bond lengths involving hydrogen atoms were fixed using the SHAKE algorithm . The system was equilibrated for 5 ns using an NPT ensemble at 1 atm pressure and 310 K temperature with constraints, the production simulations were carried out for 300 ns without any constraints, and the trajectory was saved for every 10 picoseconds.

References

1. Schneider, W. M., Chevillotte, M. D. & Rice, C. M. Interferon-Stimulated Genes: A Complex Web of Host Defenses. *Annu. Rev. Immunol.* **32**, 513–545 (2014).
2. Perng, Y.-C. & Lenschow, D. J. ISG15 in antiviral immunity and beyond. *Nat. Rev. Microbiol.* **16**, 423–439 (2018).
3. Kim, K. I., Giannakopoulos, N. V., Virgin, H. W. & Zhang, D.-E. Interferon-Inducible Ubiquitin E2, Ubc8, Is a Conjugating Enzyme for Protein ISGylation. *Mol. Cell. Biol.* **24**, 9592–9600 (2004).
4. Kok, K. *et al.* A gene in the chromosomal region 3p21 with greatly reduced expression in lung cancer is similar to the gene for ubiquitin-activating enzyme. *Proc. Natl. Acad. Sci.* **90**, 6071–6075 (1993).
5. Wong, J. J. Y., Pung, Y. F., Sze, N. S.-K. & Chin, K.-C. HERC5 is an IFN-induced HECT-type E3 protein ligase that mediates type I IFN-induced ISGylation of protein targets. *Proc. Natl. Acad. Sci.* **103**, 10735–10740 (2006).
6. D'Cunha, J., Knight, E., Haas, A. L., Truitt, R. L. & Borden, E. C. Immunoregulatory properties of ISG15, an interferon-induced cytokine. *Proc. Natl. Acad. Sci. U. S. A.* **93**, 211–215 (1996).
7. Swaim, C. D. *et al.* Modulation of Extracellular ISG15 Signaling by Pathogens and Viral Effector Proteins. *Cell Rep.* **31**, 107772 (2020).
8. Swaim, C. D., Scott, A. F., Canadeo, L. A. & Huibregtse, J. M. Extracellular ISG15 Signals Cytokine Secretion through the LFA-1 Integrin Receptor. *Mol. Cell* **68**, 581-590.e5 (2017).

9. D'Cunha, J., Knight, E., Haas, A. L., Truitt, R. L. & Borden, E. C. Immunoregulatory properties of ISG15, an interferon-induced cytokine. *Proc. Natl. Acad. Sci.* **93**, 211–215 (1996).

10. Liu, G. *et al.* ISG15-dependent activation of the sensor MDA5 is antagonized by the SARS-CoV-2 papain-like protease to evade host innate immunity. *Nat. Microbiol.* **6**, 467–478 (2021).

11. Munnur, D. *et al.* Altered ISGylation drives aberrant macrophage-dependent immune responses during SARS-CoV-2 infection. *Nat. Immunol.* 1–12 (2021) doi:10.1038/s41590-021-01035-8.

12. Zaheer, R. S. *et al.* Human rhinovirus-induced ISG15 selectively modulates epithelial antiviral immunity. *Mucosal Immunol.* **7**, 1127–1138 (2014).

13. Shin, D. *et al.* Papain-like protease regulates SARS-CoV-2 viral spread and innate immunity. *Nature* **587**, 657–662 (2020).

14. Chiok, K., Hutchison, K., Miller, L. G., Bose, S. & Miura, T. A. Proinflammatory Responses in SARS-CoV-2 and Soluble Spike Glycoprotein S1 Subunit Activated Human Macrophages. *Viruses* **15**, 754 (2023).

15. Zhou, Y. *et al.* SARS-CoV-2 Spike protein enhances ACE2 expression via facilitating Interferon effects in bronchial epithelium. *Immunol. Lett.* **237**, 33–41 (2021).

16. González-Sanz, R. *et al.* ISG15 Is Upregulated in Respiratory Syncytial Virus Infection and Reduces Virus Growth through Protein ISGylation. *J. Virol.* **90**, 3428–3438 (2016).

17. Chiok, K. *et al.* Human Respiratory Syncytial Virus NS2 Protein Induces Autophagy by Modulating Beclin1 Protein Stabilization and ISGylation. *mBio* **13**, e03528-21 (2022).

18. Bogunovic, D., Boisson-Dupuis, S. & Casanova, J.-L. ISG15: leading a double life as a secreted molecule. *Exp. Mol. Med.* **45**, e18–e18 (2013).

19. Napolitano, A. *et al.* Cysteine-Reactive Free ISG15 Generates IL-1β–Producing CD8α+ Dendritic Cells at the Site of Infection. *J. Immunol.* **201**, 604–614 (2018).

20. Haas, A. L., Ahrens, P., Bright, P. M. & Ankel, H. Interferon induces a 15-kilodalton protein exhibiting marked homology to ubiquitin. *J. Biol. Chem.* **262**, 11315–11323 (1987).

21. Hynes, R. O. Integrins: Bidirectional, Allosteric Signaling Machines. *Cell* **110**, 673–687 (2002).

22. Shattil, S. J., Kim, C. & Ginsberg, M. H. The final steps of integrin activation: the end game. *Nat. Rev. Mol. Cell Biol.* **11**, 288–300 (2010).

23. Campbell, I. D. & Humphries, M. J. Integrin Structure, Activation, and Interactions. *Cold Spring Harb. Perspect. Biol.* **3**, a004994 (2011).

24. Guo, W. & Giancotti, F. G. Integrin signalling during tumour progression. *Nat. Rev. Mol. Cell Biol.* **5**, 816–826 (2004).

25. Lelièvre, S., Weaver, V. M. & Bissell, M. J. Extracellular Matrix Signaling from the Cellular Membrane Skeleton to the Nuclear Skeleton: A Model of Gene Regulation. *Recent Prog. Horm. Res.* **51**, 417–432 (1996).

26. Eke, I. *et al.* β_1 Integrin/FAK/cortactin signaling is essential for human head and neck cancer resistance to radiotherapy. *J. Clin. Invest.* **122**, 1529–1540 (2012).

27. Guan, J.-L. Role of focal adhesion kinase in integrin signaling. *Int. J. Biochem. Cell Biol.* **29**, 1085–1096 (1997).

28. Lee, C. C., Carette, J. E., Brummelkamp, T. R. & Ploegh, H. L. A Reporter Screen in a Human Haploid Cell Line Identifies CYLD as a Constitutive Inhibitor of NF-κB. *PLoS ONE* **8**, e70339 (2013).

29. Pokharel, S. M. *et al.* Integrin activation by the lipid molecule 25-hydroxycholesterol induces a proinflammatory response. *Nat. Commun.* **10**, 1482 (2019).

30. Ludwig, B. S., Kessler, H., Kossatz, S. & Reuning, U. RGD-Binding Integrins Revisited: How Recently Discovered Functions and Novel Synthetic Ligands (Re-)Shape an Ever-Evolving Field. *Cancers* **13**, 1711 (2021).

31. Sarin, V., Gaffin, R. D., Meininger, G. A. & Muthuchamy, M. Arginine–glycine–aspartic acid (RGD)-containing peptides inhibit the force production of mouse papillary muscle bundles via α5β1 integrin. *J. Physiol.* **564**, 603–617 (2005).

32. Sasamoto, A. *et al.* Mechanotransduction by integrin is essential for IL-6 secretion from endothelial cells in response to uniaxial continuous stretch. *Am. J. Physiol.-Cell Physiol.* **288**, C1012–C1022 (2005).

33. Mogford, J. E., Davis, G. E. & Meininger, G. A. RGDN peptide interaction with endothelial alpha5beta1 integrin causes sustained endothelin-dependent vasoconstriction of rat skeletal muscle arterioles. *J. Clin. Invest.* **100**, 1647–1653 (1997).

34. Ley, K., Rivera-Nieves, J., Sandborn, W. J. & Shattil, S. Integrin-based Therapeutics: Biological Basis, Clinical Use and New Drugs. *Nat. Rev. Drug Discov.* **15**, 173–183 (2016).

35. Schumacher, S. *et al.* Structural insights into integrin α5β1 opening by fibronectin ligand. *Sci. Adv.* **7**, eabe9716 (2021).

36. Lin, F.-Y., Zhu, J., Eng, E. T., Hudson, N. E. & Springer, T. A. β-Subunit Binding Is Sufficient for Ligands to Open the Integrin αIIbβ3 Headpiece. *J. Biol. Chem.* **291**, 4537–4546 (2016).

37. Arimori, T. *et al.* Structural mechanism of laminin recognition by integrin. *Nat. Commun.* **12**, 4012 (2021).

38. Narasimhan, J. *et al.* Crystal structure of the interferon-induced ubiquitin-like protein ISG15. *J. Biol. Chem.* **280**, 27356–27365 (2005).

39. Swaim, C. D. *et al. 6-Thioguanine Blocks SARS-CoV-2 Replication by Inhibition of PLpro Protease Activities*. http://biorxiv.org/lookup/doi/10.1101/2020.07.01.183020 (2020) doi:10.1101/2020.07.01.183020.

40. Leite, W. C. *et al.* Conformational Dynamics in the Interaction of SARS-CoV-2 Papain-like Protease with Human Interferon-Stimulated Gene 15 Protein. *J. Phys. Chem. Lett.* **12**, 5608–5615 (2021).

41. Cao, X. ISG15 secretion exacerbates inflammation in SARS-CoV-2 infection. *Nat. Immunol.* **22**, 1360–1362 (2021).

42. Dos Santos, P. F. *et al.* ISG15-Induced IL-10 Is a Novel Anti-Inflammatory Myeloid Axis Disrupted during Active Tuberculosis. *J. Immunol.* **200**, 1434–1442 (2018).

43. Bailly, P., Tontti, E., Hermand, P., Cartron, J.-P. & Gahmberg, C. G. The red cell LW blood group protein is an intercellular adhesion molecule which binds to CD11/CD18 leukocyte integrins. *Eur. J. Immunol.* **25**, 3316–3320 (1995).

44. Teoh, C. M., Tan, S. S. L. & Tran, T. Integrins as Therapeutic Targets for Respiratory Diseases. *Curr. Mol. Med.* **15**, 714 (2016).

45. Hocking, D. C. Fibronectin matrix deposition and cell contractility: implications for airway remodeling in asthma. *Chest* **122**, 275S-278S (2002).

46. White, E. S. *et al.* Integrin alpha4beta1 regulates migration across basement membranes by lung fibroblasts: a role for phosphatase and tensin homologue deleted on chromosome 10. *Am. J. Respir. Crit. Care Med.* **168**, 436–442 (2003).

47. Grassmé, H. *et al.* β1-Integrin Accumulates in Cystic Fibrosis Luminal Airway Epithelial Membranes and Decreases Sphingosine, Promoting Bacterial Infections. *Cell Host Microbe* **21**, 707-718.e8 (2017).

48. Schumacher, S. *et al.* Structural insights into integrin α5β1 opening by fibronectin ligand. *Sci. Adv.* **7**, eabe9716 (2021).

49. Legate, K. R., Wickström, S. A. & Fässler, R. Genetic and cell biological analysis of integrin outside-in signaling. *Genes Dev.* **23**, 397–418 (2009).

50. Xie, B. *et al.* Focal adhesion kinase activates Stat1 in integrin-mediated cell migration and adhesion. *J. Biol. Chem.* **276**, 19512–19523 (2001).

51. Bozym, R. A. *et al.* Focal Adhesion Kinase Is a Component of Antiviral RIG-I-like Receptor Signaling. *Cell Host Microbe* **11**, 153–166 (2012).

52. Elbahesh, H. *et al.* Novel Roles of Focal Adhesion Kinase in Cytoplasmic Entry and Replication of Influenza A Viruses. *J. Virol.* **88**, 6714–6728 (2014).

53. DeFilippis, V. R. *et al.* Interferon Regulatory Factor 3 Is Necessary for Induction of Antiviral Genes during Human Cytomegalovirus Infection. *J. Virol.* **80**, 1032–1037 (2006).

54. Bianco, C. & Mohr, I. Restriction of Human Cytomegalovirus Replication by ISG15, a Host Effector Regulated by cGAS-STING Double-Stranded-DNA Sensing. *J. Virol.* **91**, e02483-16 (2017).

55. Transcription Factor Redundancy Ensures Induction of the Antiviral State - PMC. https://www.ncbi.nlm.nih.gov/pmc/articles/PMC3009927/.

56. Radoshevich, L. *et al.* ISG15 counteracts Listeria monocytogenes infection. *eLife* **4**, e06848 (2015).

57. Ning, S., Pagano, J. S. & Barber, G. N. IRF7: activation, regulation, modification and function. *Genes Immun.* **12**, 399–414 (2011).

58. Au, W.-C., Moore, P. A., LaFleur, D. W., Tombal, B. & Pitha, P. M. Characterization of the Interferon Regulatory Factor-7 and Its Potential Role in the Transcription Activation of Interferon A Genes *. *J. Biol. Chem.* **273**, 29210–29217 (1998).

59. Schornberg, K. L. *et al.* α5β1-Integrin controls ebolavirus entry by regulating endosomal cathepsins. *Proc. Natl. Acad. Sci. U. S. A.* **106**, 8003–8008 (2009).

60. Tugizov, S. M., Berline, J. W. & Palefsky, J. M. Epstein-Barr virus infection of polarized tongue and nasopharyngeal epithelial cells. *Nat. Med.* **9**, 307–314 (2003).

61. Jackson, T. *et al.* Foot-and-mouth disease virus is a ligand for the high-affinity binding conformation of integrin alpha5beta1: influence of the leucine residue within the RGDL motif on selectivity of integrin binding. *J. Gen. Virol.* **81**, 1383–1391 (2000).

62. Shang, J. *et al.* Structural basis of receptor recognition by SARS-CoV-2. *Nature* **581**, 221–224 (2020).

63. Potter, J. L., Narasimhan, J., Mende-Mueller, L. & Haas, A. L. Precursor Processing of Pro-ISG15/UCRP, an Interferon-β-induced Ubiquitin-like Protein *. *J. Biol. Chem.* **274**, 25061–25068 (1999).

64. Segovia, J. *et al.* TLR2/MyD88/NF-κB Pathway, Reactive Oxygen Species, Potassium Efflux Activates NLRP3/ASC Inflammasome during Respiratory Syncytial Virus Infection. *PLoS ONE* **7**, e29695 (2012).

65. Segovia, J. A. *et al.* Nedd8 Regulates Inflammasome-Dependent Caspase-1 Activation. *Mol. Cell. Biol.* **35**, 582–597 (2015).

66. Sabbah, A. *et al.* Activation of innate immune antiviral responses by Nod2. *Nat. Immunol.* **10**, 1073–1080 (2009).

67. Pokharel, S. M. *et al.* Integrin activation by the lipid molecule 25-hydroxycholesterol induces a proinflammatory response. *Nat. Commun.* **10**, 1482 (2019).

68. Hotard, A. L. *et al.* A Stabilized Respiratory Syncytial Virus Reverse Genetics System Amenable to Recombination Mediated Mutagenesis. *Virology* **434**, 129–136 (2012).

69. Meng, J., Lee, S., Hotard, A. L. & Moore, M. L. Refining the Balance of Attenuation and Immunogenicity of Respiratory Syncytial Virus by Targeted Codon Deoptimization of Virulence Genes. *mBio* **5**, e01704-14 (2014).

70. Burley, S. K. *et al.* RCSB Protein Data Bank (RCSB.org): delivery of experimentally-determined PDB structures alongside one million computed structure models of proteins from artificial intelligence/machine learning. *Nucleic Acids Res.* **51**, D488–D508 (2022).

71. Chemical Computing Group (CCG) | Computer-Aided Molecular Design. https://www.chemcomp.com/index.htm.

72. HADDOCK Web Server. https://bianca.science.uu.nl/.

73. van Zundert, G. C. P. *et al.* The HADDOCK2.2 Web Server: User-Friendly Integrative Modeling of Biomolecular Complexes. *J. Mol. Biol.* **428**, 720–725 (2016).

74. Case, D. A. *et al.* The Amber biomolecular simulation programs. *J. Comput. Chem.* **26**, 1668–1688 (2005).

75. Suh, D. *et al.* CHARMM-GUI Enhanced Sampler for various collective variables and enhanced sampling methods. *Protein Sci. Publ. Protein Soc.* **31**, e4446 (2022).

76. Jorgensen, W. L., Chandrasekhar, J., Madura, J. D., Impey, R. W. & Klein, M. L. Comparison of simple potential functions for simulating liquid water. *J. Chem. Phys.* **79**, 926–935 (1983).

77. Darden, T., York, D. & Pedersen, L. Particle mesh Ewald: An N·log(N) method for Ewald sums in large systems. *J. Chem. Phys.* **98**, 10089–10092 (1993).

78. Harvey, M. J. & De Fabritiis, G. An Implementation of the Smooth Particle Mesh Ewald Method on GPU Hardware. *J. Chem. Theory Comput.* **5**, 2371–2377 (2009).

79. Andersen, H. C. Rattle: A “velocity” version of the shake algorithm for molecular dynamics calculations. *J. Comput. Phys.* **52**, 24–34 (1983).

Figure Legends

Figure 1. SARS-CoV-2 S protein induces expression of intracellular ISG15, ISGylation, and extracellular release of ISG15 in epithelial cells. A) Human lung epithelial Calu-3 cells were infected with SARS-CoV-2 (MOI= 0.1). Whole cell lysate (WCL) collected at 48h post-infection (hpi) and 120hpi was subjected to immunoblotting with ISG15, PLpro and actin antibodies. B) Cell culture supernatants (supernatant) from SARS-CoV-2 (MOI= 0.1) infected Calu-3 cells were collected at 120 hours post infection. Trichloroacetic acid (TCA) precipitated supernatant was subjected to immunoblot with anti-ISG15 antibody to detect extracellular ISG15. C) Supernatants from mock and SARS-CoV-2 infected (120 hpi) Calu-3 cells were used to quantify cell death by lactate dehydrogenase (LDH) assay. D) Experimental schematic – human lung epithelial A549 cells were transfected with either plasmids encoding C9-tagged S proteins from various coronaviruses or empty vector control plasmid pcDNA 3.1 (pcDNA). At 24h post-transfection, washed cells were incubated with fresh media without plasmids for 16h and 24h. Whole cell lysate (WCL) was collected for analysis. E) WCL collected from A549 cells transfected with C9-tagged SARS-CoV-2 (SARS2) S protein as described in the experimental schematic in Fig. 1D was subjected to immunoblotting with ISG15, C9, and actin antibodies. A549 cells treated with interferon-β (IFN-β, 100U/mL) for 24 was used as a positive control for ISGylation. F) A549 cells were transfected with C9-tagged S protein from various coronaviruses including MERS-CoV (MERS), 229E, SARS-CoV-2 (SARS2) and SARS-CoV-1 (SARS1) or empty vector control (pcDNA). The experiment was conducted as described in the experimental scheme shown in Fig. 1D. WCL collected at 24h was subjected to immunoblotting with ISG15, C9, and actin antibodies. G) Experimental schematic - A549 cells were transfected with either plasmid encoding C9-tagged SARS-CoV-2 S protein or empty vector control (pcDNA). At 24h post-transfection, washed cells were incubated with fresh media without plasmids for 8h, 16h and 24h. Total protein in plasmid-free culture supernatant was precipitated with TCA. H) TCA precipitated culture supernatant collected from A549 cells transfected with C9-tagged SARS-CoV-2 (SARS2) S protein as described in the experimental schematic in Fig. 1G was subjected to immunoblotting with ISG15 antibody to detect extracellularly released ISG15.

Figure 2. Respiratory Syncytial virus (RSV) induces ISGylation and extracellular release of ISG15 from epithelial cells. A) Human lung epithelial A549 cells were infected with RSV expressing mKate2 protein (MOI=0.1). WCL collected at 48h post-infection was subjected to immunoblotting with ISG15, RFP (to detect mKate2 protein) and actin antibodies. B) Cell culture supernatants from A549 cells infected with RSV as described in Fig. 2A were precipitated with TCA and total protein was immunoblotted with ISG15 antibody to detect extracellular ISG15. C) Supernatants from mock and RSV infected (48h post-infection) A549 cells were used to quantify cell death by lactate dehydrogenase (LDH) assay.

Figure 3. **Extracellular ISG15 induces intracellular ISG15 and ISGylation: upregulation of intracellular ISG15 protein in uninfected bystander cells during virus infection.** Human lung epithelial A549 (A) and Calu-3 (B) cells were treated with purified recombinant ISG15 protein (rISG15, 5µg/mL) for the indicated times and WCL was immunoblotted with ISG15 and actin antibodies. C) Fluorescence microscopic image of A549 cells mock-infected or infected with mKate2-RSV (MOI=0.1). Cells were labelled with ISG15 antibody and FITC (green) to detect endogenous ISG15 protein. Nuclei were stained with DAPI (blue). Infected cells were visualized by the red fluorescence emitted from the mKate2 protein.

Figure 4. Extracellular ISG15 induces intracellular ISG15 protein and ISGylation via a type-I interferon (IFN) independent mechanism. A) 2fTGH (IFN-competent) and U5A (IFN-incompetent) cells were treated with purified recombinant ISG15 protein (rISG15, 5µg/mL) for 6h before collection of WCL for immunoblotting with ISG15 and actin antibodies. B) VeroE6 cells (IFN-incompetent) were treated with rISG15 (5µg/mL) for 6h before collection of WCL for immunoblotting with ISG15 and actin antibodies. C) VeroE6 cells were infected with mKate2-RSV (MOI=0.1) for 48h before WCL collection for immunoblotting with ISG15, RFP (to detect mKate2) and actin antibodies. D) Cell culture supernatants from VeroE6 cells infected with RSV as described in Fig. 4C were precipitated with TCA and total protein was immunoblotted with ISG15 antibody to detect extracellular ISG15. E) Fluorescence microscopic image of VeoE6 cells mock-infected or infected with mKate2-RSV (MOI=0.1). Cells were labelled with ISG15 antibody and FITC (green) to detect endogenous ISG15 protein. Nuclei were stained with DAPI (blue). Infected cells were visualized by the red fluorescence emitted from the mKate2 protein.

Figure 5. Antiviral activity of extracellular ISG15 protein: IFN-independent antiviral response by extracellular ISG15. A) VeroE6 cells were pre-treated with purified recombinant ISG15 protein (rISG15, 5µg/mL) or vehicle control for 8 hours prior to infection with mKate2-RSV for 48h before collection of WCL for immunoblotting with RFP (to detect mKate2) and actin antibodies. B) Bright field microscopy of VeroE6 monolayers treated with vehicle control or rISG15 prior to infection with RSV (MOI=1, 16h). C) Infectious viral titer following RSV (MOI=0.1) infection of VeroE6 cells pre-treated with either vehicle control or rISG15 (5µg/mL). D) Infectious viral titer following RSV infection (MOI=0.1, 16h) of VeoE6 cells in the presence of either control IgG or anti-ISG15 antibody (Ab). E) VeoE6 cells pre-treated with either control IgG or anti-ISG15 antibody was infected with RSV (MOI=0.1, 48h). WCL collected from the cells were subjected to immunoblotting with RFP (to detect mKate2) and actin antibodies. *$p < 0.05$ & **$p < 0.01$ using a Student's t-test.

Figure 6. Extracellular ISG15 induces intracellular ISG15 for ISGylation via integrin-FAK pathway: interaction of ISG15 with α5β1 integrin. A) Cell lysate from A549 cells incubated with purified recombinant ISG15 protein (rISG15, 5µg/mL) or vehicle for 4h at 4°C were immune-precipitated (IP) with ISG15 antibody and subsequently immuno-blotted (IB) with α5 integrin antibody. WCL were also blotted with α5 integrin and actin antibodies. B) Biotinylated purified α5β1 integrin protein (5.7 mM) or biotinylatedvehicle (control was incubated with rISG15 protein (0.1 µM) for 16h at 4°C. Following incubation, biotinylated molecules were precipitated with avidin-agarose beads and the avidin-agarose bound complex was immune-blotted (IB) with ISG15 antibody. C) WCL from A549 cells incubated with either rISG15 (1µg/mL) or vehicle for 15 minutes (15m) or 30m were subjected to immunoblotting with phospho-FAK antibody that detects Tyr925 phosphorylation of activated FAK. WCL was also immunoblotted with FAK and actin antibodies. D) A549 cells were treated with rISG15 (1µg/mL) in the presence of either vehicle control or FAK inhibitor (FAKi, 20 µM). WCL collected from these cells were subjected to immunoblotting with ISG15 antibody to detect unconjugated monomeric form of ISG15. E) A549 cells were treated with rISG15 (1µg/mL) in the presence of either vehicle control or FAK inhibitor (FAKi, 20 µM). WCL collected from these cells were subjected to immunoblotting with ISG15 antibody to detect ISGylated proteins. F) Wild type (WT) and α5 integrin KO (ITGA5 KO) HAP1 cells were treated with rISG15

(5ug/mL). WCL collected from these cells were subjected to immunoblotting with ISG15 antibody. G) A549 cells were treated with rISG15 (2µg/mL) in the presence of either control peptide or RGD peptide (200 µM). Cells were also treated with rISG15 in the absence of any peptide (untreated cells). WCL collected from these cells were subjected to immunoblotting with ISG15 antibody to detect ISGylated proteins. H) A549 cells were treated with rISG15 (2µg/mL) in the presence of either control peptide or RGD peptide (200 µM). Cells were also treated with rISG15 in the absence of any peptide (untreated cells). WCL collected from these cells were subjected to immunoblotting with ISG15 antibody to detect unconjugated monomeric form of ISG15.

Figure 7. Molecular modeling of extracellular ISG15- α5β1 integrin interaction. A) Crystal structure of α5β1 integrin bound with fibronectin (PDB ID: 7NWL). B) RGD motif binding site at the integrin α5β1 integrin headpiece. RGD residues of fibronectin are shown as licorice, while β-propeller of α5 and βI domain of β1 subunits are shown as cartoon representation. C) Crystal structure of ISG15 (PDB ID: 3RT3). D) Docked orientation of ISG15 with integrin α5β1. E) Residues of ISG15 binding with the RGD motif binding site of α5β1 integrin are shown as orange-colored sticks. F) Superposition of fibronectin RGD residues with the residues of ISG15. Arg99 of ISG15 is positioned similar to the arginine (RGD) of fibronectin and Glu80 occupies the aspartic acid (RGD) binding site. G) Integrin α5β1's activation-specific interactions with ISG15. Please make (F) and (G) clearer.

Figure 8. Schematic model showing antiviral pro-ISGylation activity of extracellular ISG15 via a type-I interferon (IFN) independent mechanism. Virus infection will trigger intracellular buildup of cellular unconjugated ISG15 protein, which will be utilized for ISGylation. A portion of unconjugated ISG15 will be released from infected cells. Extracellular ISG15 will interact with the cell surface integrin molecules of uninfected bystander cells (paracrine action) to trigger FAK-dependent intracellular ISG15 induction and subsequent ISGylation via an IFN independent mechanism. Since ISGylation possesses antiviral activity, it will confer an antiviral state in the uninfected bystander cells to ensure reduced viral infectivity during subsequent infection of these cells. Apart from paracrine action, extracellular ISG15 can also act on infected cells (autocrine action) for optimal antiviral response.

Fig. 1

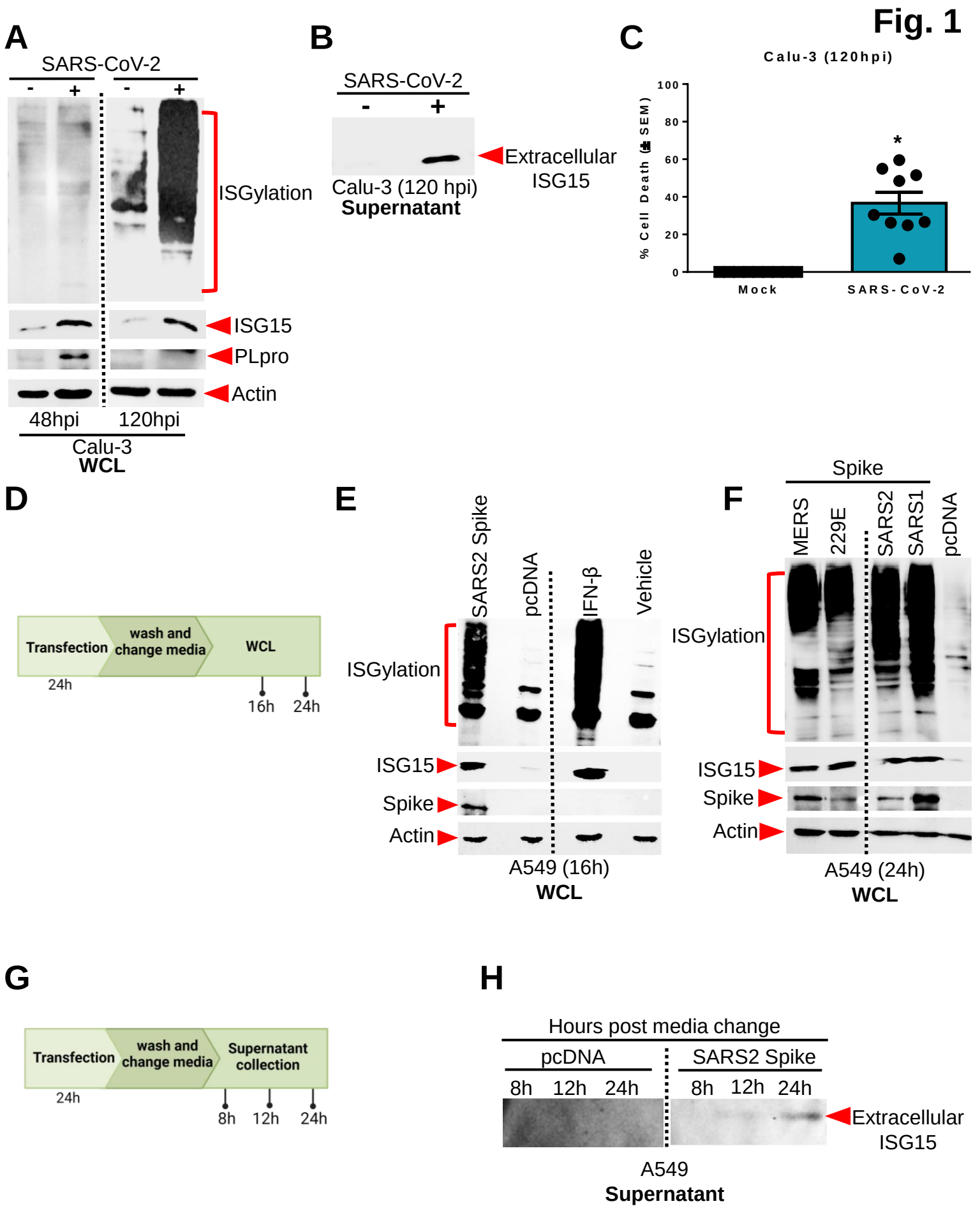
A
SARS-CoV-2
-
+
-
+
ISGylation
ISG15
PLpro
Actin
48hpi
120hpi
Calu-3
WCL
B
SARS-CoV-2
-
+
Extracellular ISG15
Calu-3 (120 hpi)
Supernatant
C
Calu-3 (120hpi)
% Cell Death (± SEM)
100
80
60
40
20
0
*
Mock
SARS-CoV-2
D
Transfection
wash and change media
WCL
24h
16h
24h
E
SARS2 Spike
pcDNA
IFN-β
Vehicle
ISGylation
ISG15
Spike
Actin
A549 (16h)
WCL
F
Spike
MERS
229E
SARS2
SARS1
pcDNA
ISGylation
ISG15
Spike
Actin
A549 (24h)
WCL
G
Transfection
wash and change media
Supernatant collection
24h
8h
12h
24h
H
Hours post media change
pcDNA
SARS2 Spike
8h
12h
24h
8h
12h
24h
Extracellular ISG15
A549
Supernatant

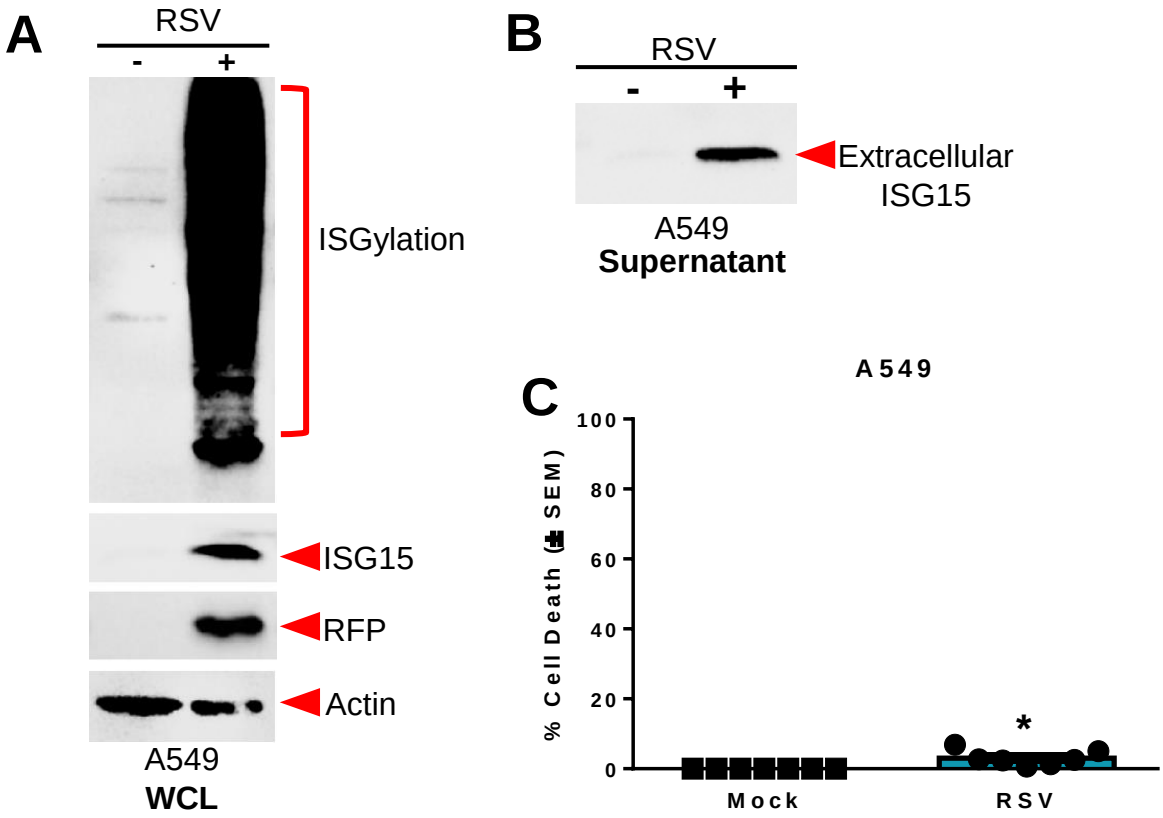
A
RSV
-
+
ISGylation
ISG15
RFP
Actin
A549
WCL
B
RSV
-
+
Extracellular
ISG15
A549
Supernatant
C
A549
% Cell Death (± SEM)
100
80
60
40
20
0
*
Mock
RSV

Fig. 2

Fig. 3

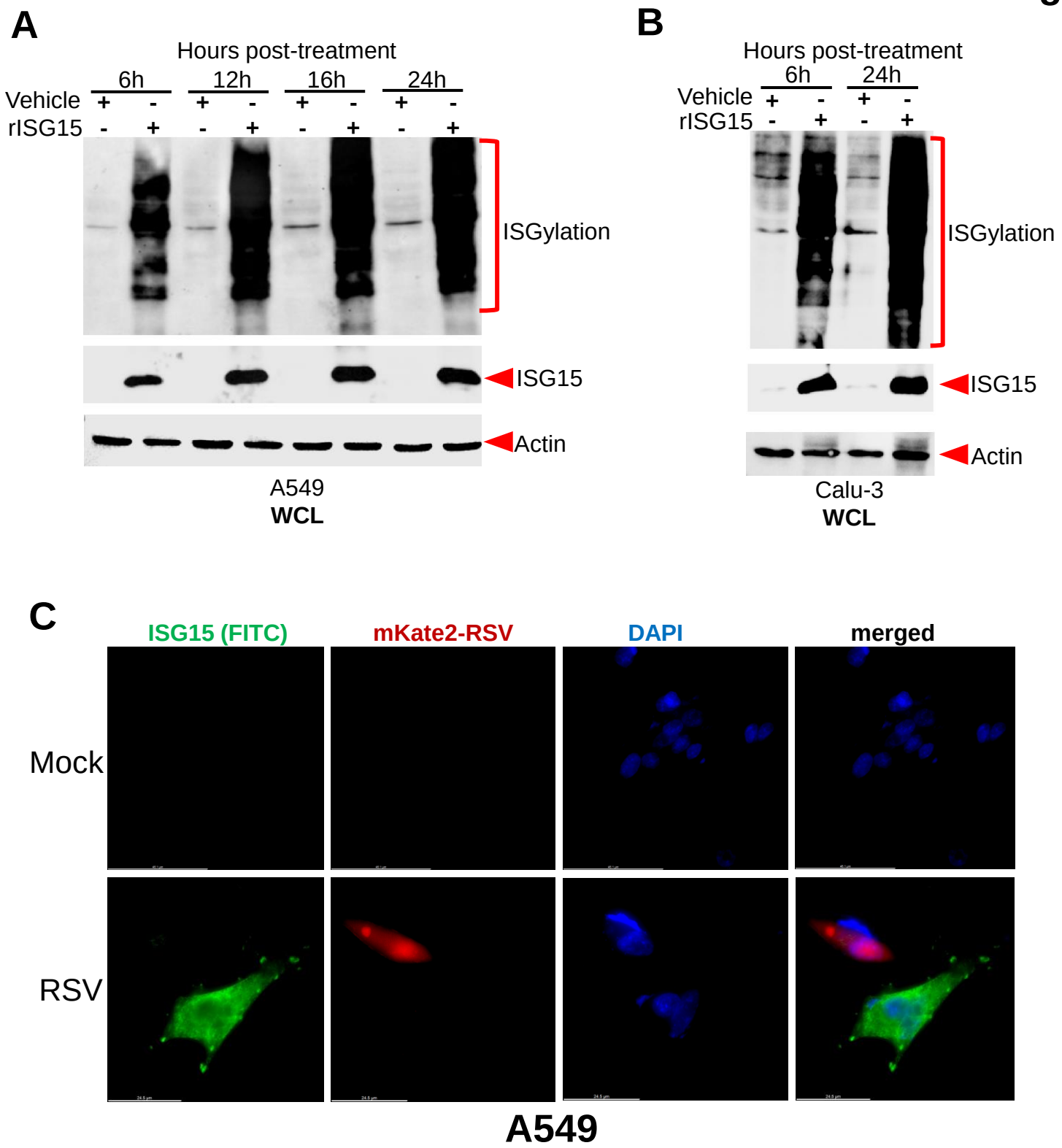
A
Hours post-treatment
6h
12h
16h
24h
Vehicle
rISG15
ISGylation
ISG15
Actin
A549
WCL
B
Hours post-treatment
6h
24h
Vehicle
rISG15
ISGylation
ISG15
Actin
Calu-3
WCL
C
ISG15 (FITC)
mKate2-RSV
DAPI
merged
Mock
RSV
A549

Fig. 4

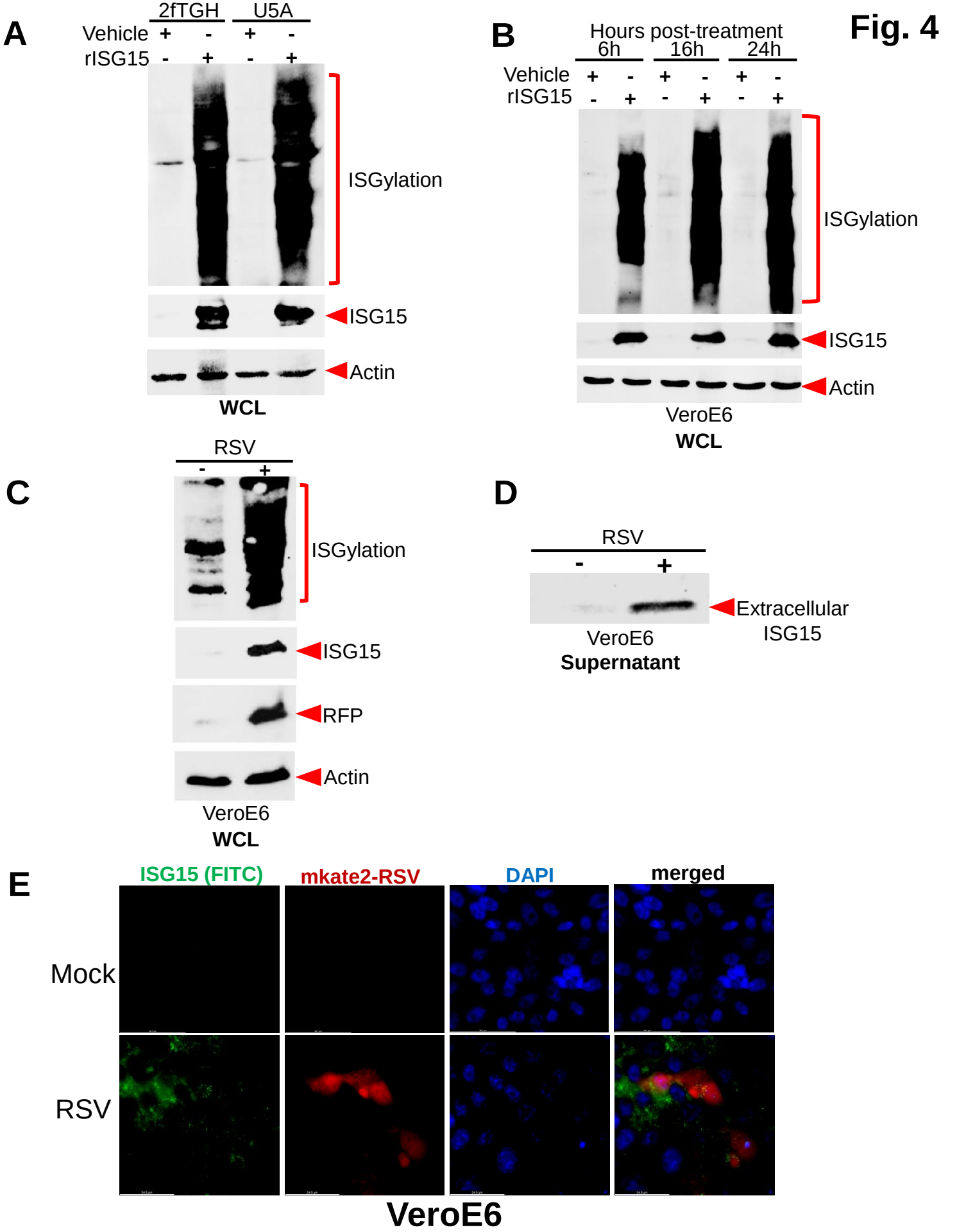
A
2fTGH
U5A
Vehicle + - + -
rISG15 - + - +
ISGylation
ISG15
Actin
WCL
B
Hours post-treatment
6h
16h
24h
Vehicle + - + - + -
rISG15 - + - + - +
ISGylation
ISG15
Actin
VeroE6
WCL
C
RSV
- +
ISGylation
ISG15
RFP
Actin
VeroE6
WCL
D
RSV
- +
Extracellular ISG15
VeroE6
Supernatant
E
ISG15 (FITC)
mkate2-RSV
DAPI
merged
Mock
RSV
VeroE6

Fig. 5

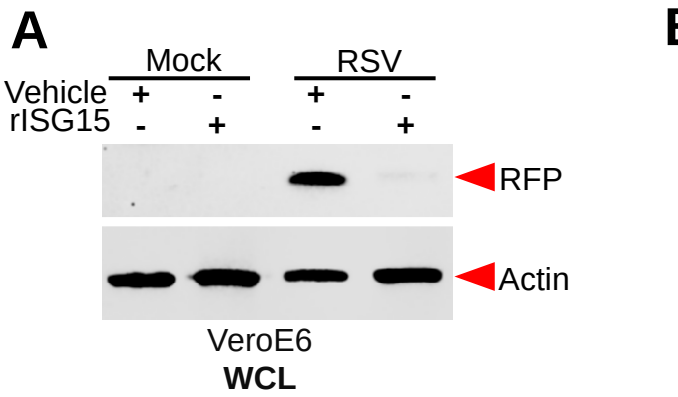
A
Mock
RSV
Vehicle + - + -
rISG15 - + - +
RFP
Actin
VeroE6
WCL

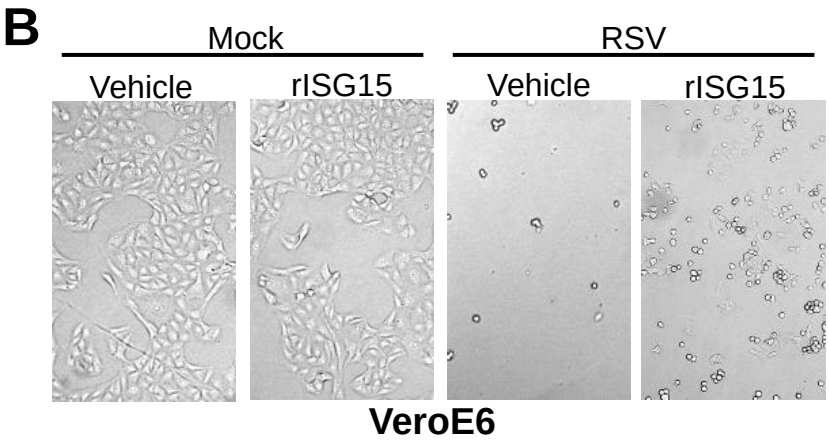
B
Mock
RSV
Vehicle
rISG15
Vehicle
rISG15
VeroE6

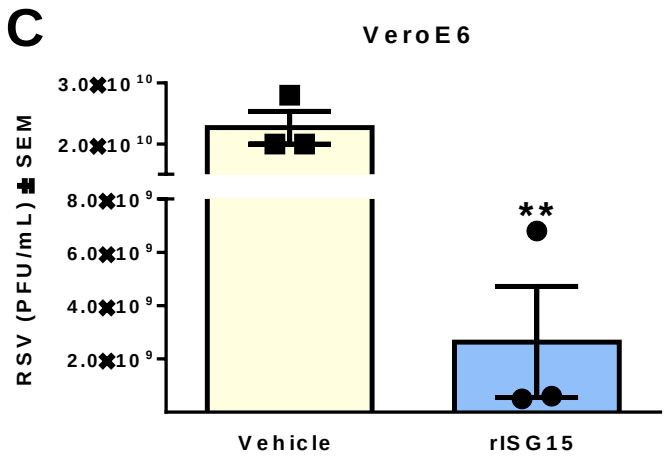
C
VeroE6
RSV (PFU/mL) ± SEM
3.0×10 10
2.0×10 10
8.0×10 9
6.0×10 9
4.0×10 9
2.0×10 9
**
Vehicle
rISG15

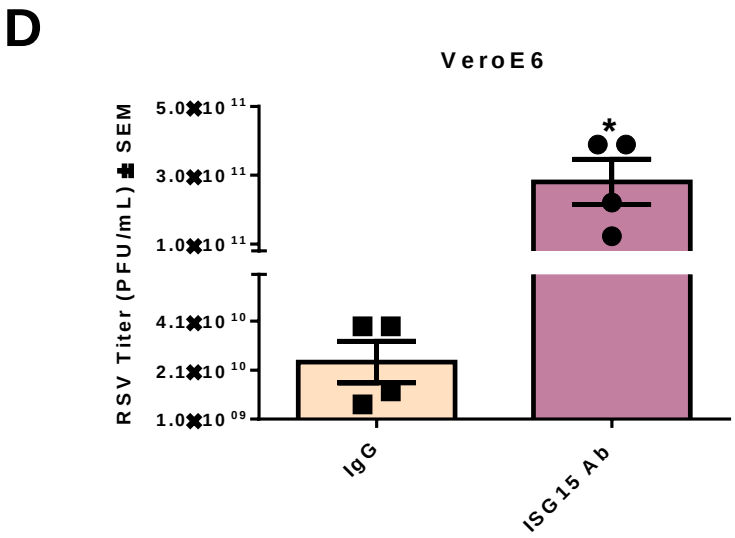
D
VeroE6
RSV Titer (PFU/mL) ± SEM
5.0×10 11
3.0×10 11
1.0×10 11
4.1×10 10
2.1×10 10
1.0×10 09
*
IgG
ISG15 Ab

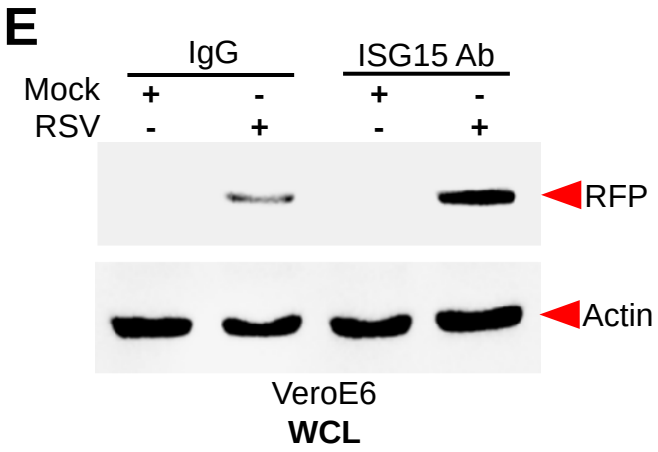
E
IgG
ISG15 Ab
Mock + - + -
RSV - + - +
RFP
Actin
VeroE6
WCL

Fig. 6

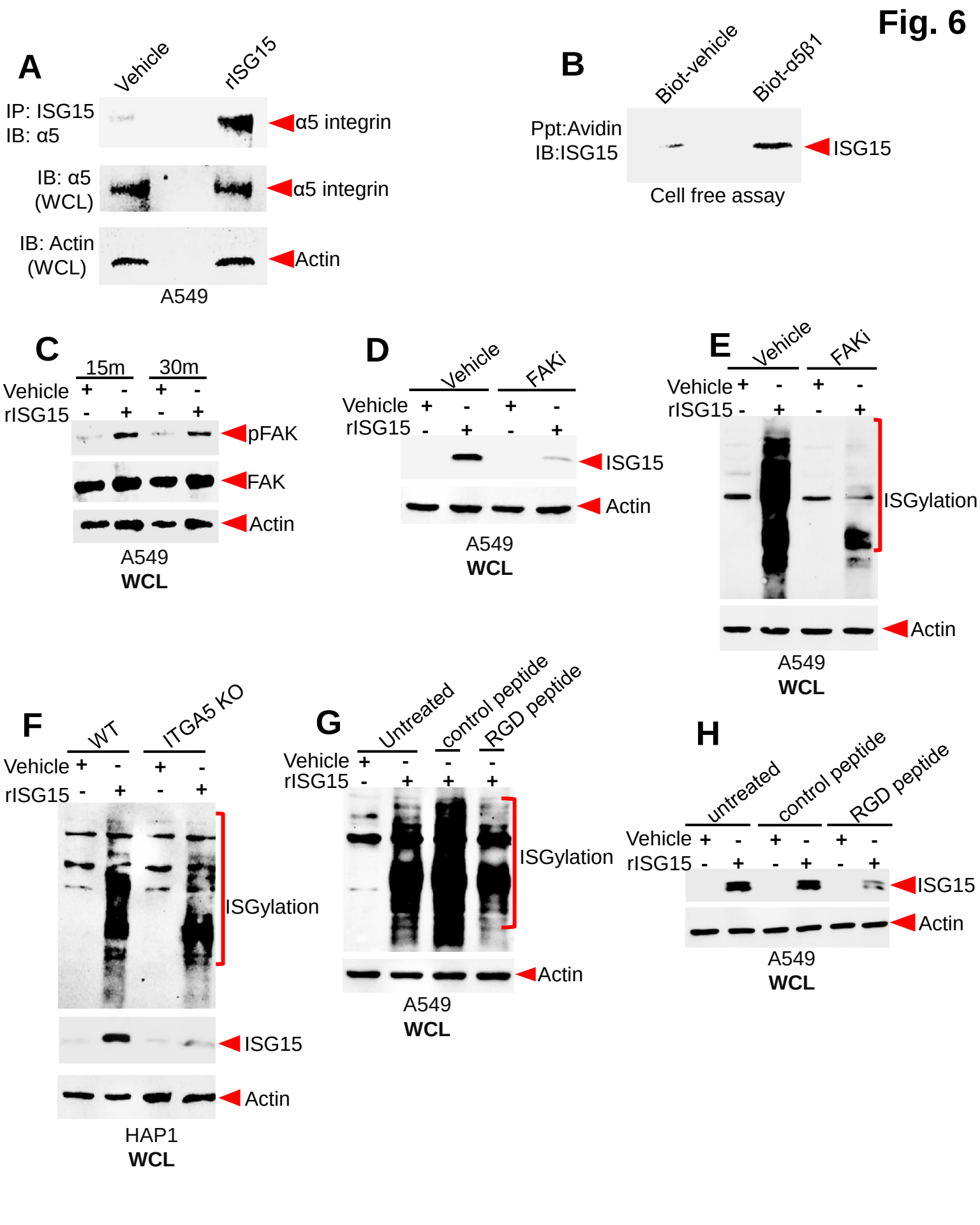
A
Vehicle
rISG15
IP: ISG15
IB: α5
α5 integrin
IB: α5
(WCL)
α5 integrin
IB: Actin
(WCL)
Actin
A549
B
Biot-vehicle
Biot-α5β1
Ppt:Avidin
IB:ISG15
ISG15
Cell free assay
C
15m
30m
Vehicle
rISG15
pFAK
FAK
Actin
A549
WCL
D
Vehicle
FAKi
Vehicle
rISG15
ISG15
Actin
A549
WCL
E
Vehicle
FAKi
Vehicle
rISG15
ISGylation
Actin
A549
WCL
F
WT
ITGA5 KO
Vehicle
rISG15
ISGylation
ISG15
Actin
HAP1
WCL
G
Untreated
control peptide
RGD peptide
Vehicle
rISG15
ISGylation
Actin
A549
WCL
H
untreated
control peptide
RGD peptide
Vehicle
rISG15
ISG15
Actin
A549
WCL

Fig. 7

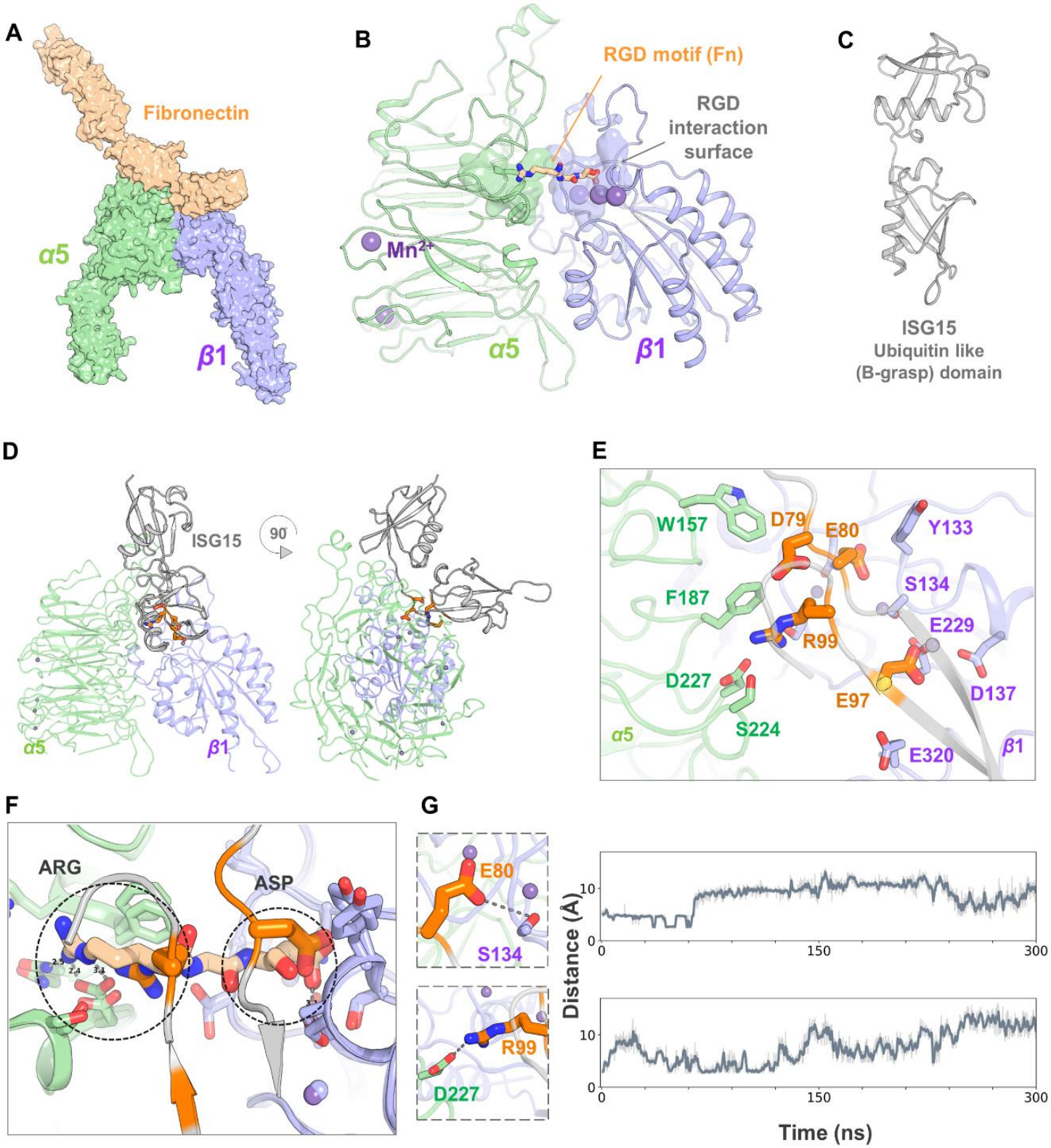
A
Fibronectin
α5
β1
B
RGD motif (Fn)
RGD interaction surface
Mn2+
α5
β1
C
ISG15
Ubiquitin like
(B-grasp) domain
D
ISG15
90
α5
β1
E
W157
D79
E80
Y133
S134
F187
E229
R99
D227
E97
D137
S224
α5
E320
β1
F
ARG
ASP
G
E80
S134
R99
D227
Distance (Å)
Time (ns)
0
150
300
10

Fig. 8

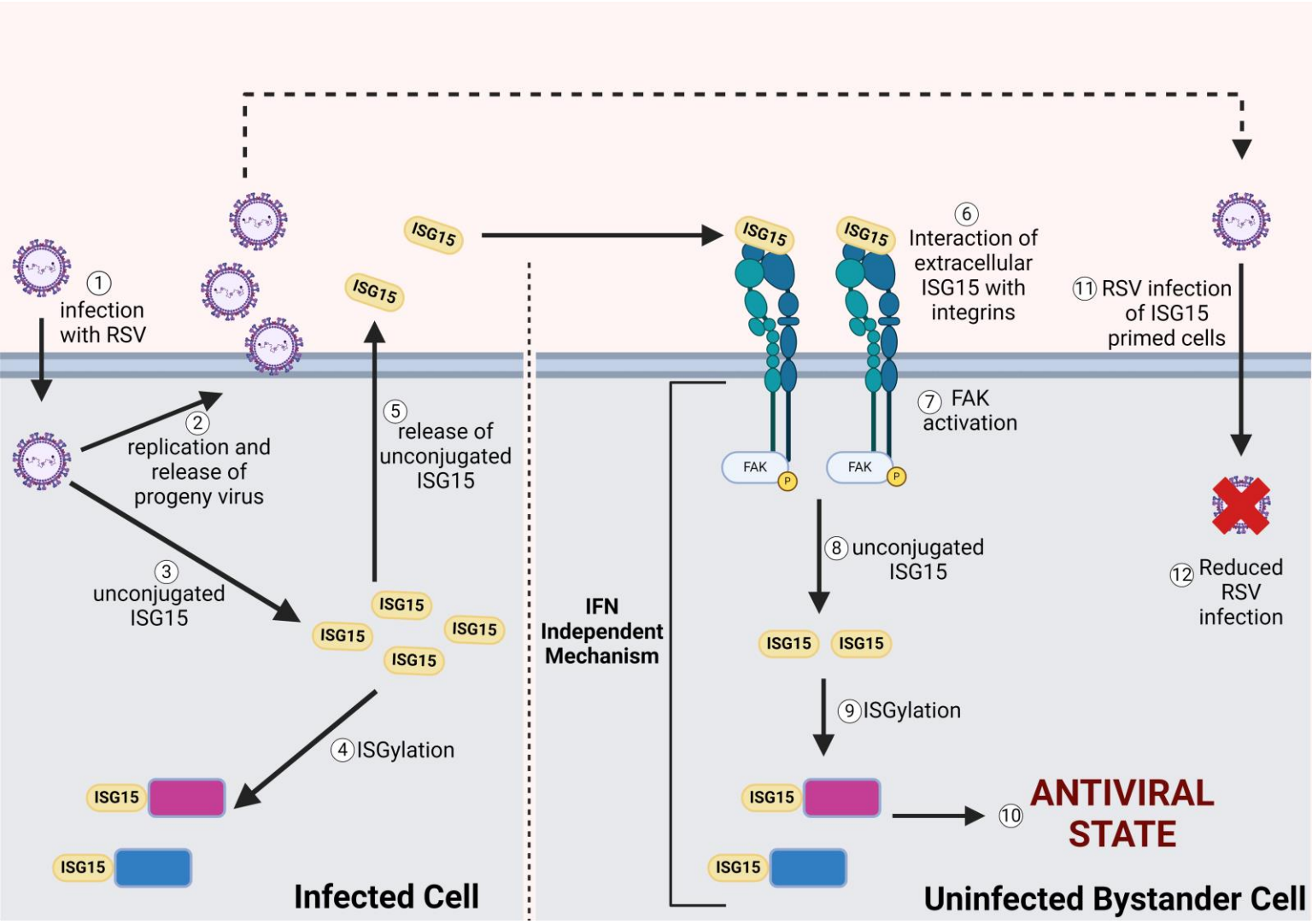
1 infection with RSV
2 replication and release of progeny virus
3 unconjugated ISG15
4 ISGylation
5 release of unconjugated ISG15
ISG15
Infected Cell
6 Interaction of extracellular ISG15 with integrins
7 FAK activation
FAK
P
8 unconjugated ISG15
9 ISGylation
10 ANTIVIRAL STATE
IFN Independent Mechanism
Uninfected Bystander Cell
11 RSV infection of ISG15 primed cells
12 Reduced RSV infection